Geochemistry, Geophysics, Geosystems

REVIEW ARTICLE

10.1002/2017GC007388

Origin of Light Noble Gases (He, Ne, and Ar) on Earth: A Review

Sandrine Péron[1], Manuel Moreira[1], and Arnaud Agranier[2]

[1]Institut de Physique du Globe de Paris - Sorbonne Paris Cité, UMR CNRS 7154, Université Paris Diderot, Paris, France, [2]Laboratoire Géosciences Océan (UMR CNRS 6538), Université de Bretagne Occidentale et Institut Universitaire Européen de la Mer, Plouzané, France

Key Points:
- The neon isotopic ratios measured in oceanic island basalts are very close to the primitive mantle neon isotopic ratios
- The solar wind implantation on preplanetesimal dust can explain the origin of light volatiles (H, He, and Ne) in the Earth's mantle
- The atmospheric neon composition is accounted for by mixing 36% of mantle neon and 64% of neon from a chondritic or cometary source

Supporting Information:
- Figure S1

Correspondence to:
S. Péron,
peron@ipgp.fr

Citation:
Péron, S., Moreira, M., & Agranier, A. (2018). Origin of light noble gases (He, Ne, and Ar) on Earth: A review. *Geochemistry, Geophysics, Geosystems*, *19*, 979–996. https://doi.org/10.1002/2017GC007388

Received 7 DEC 2017
Accepted 16 MAR 2018
Accepted article online 30 MAR 2018
Published online 13 APR 2018

Abstract We review the different scenarios for the origin of light noble gases (He, Ne, and Ar) on Earth. Several sources could have contributed to the Earth's noble gas budget: implanted solar wind, solar nebula gas, chondrites, and comets. Although there is evidence for "solar-like" neon in the Earth's mantle, questions remain as to its origin. A new compilation of noble gas data in lunar soils, interplanetary dust particles, micrometeorites, and solar wind allows examination of the implanted solar wind composition, which is key to understanding the "solar-like" mantle neon isotope composition. We show that lunar soils that reflect this solar-wind-implanted signature have a $^{20}Ne/^{22}Ne$ ratio very close to that of ocean island basalts. New data and calculations illustrate that the measured plume source $^{20}Ne/^{22}Ne$ ratio is close to the primitive mantle ratio, when taking into account mixing with the upper mantle (that has lower $^{20}Ne/^{22}Ne$ ratio). This favors early solar wind implantation to account for the origin of light volatiles (He, Ne, and possibly H) in the Earth's mantle: they were incorporated by solar wind irradiation into the Earth's precursor grains during the first few Myr of the solar system's formation. These grains must have partially survived accretion processes (only a few percent are needed to satisfy the Earth's budget of light volatiles). As for the atmosphere, the neon isotope composition can be explained by mixing 36% of mantle gases having this solar-wind-implanted signature and 64% of chondritic gases delivered in a late veneer phase.

1. Introduction

The origin of volatile elements on Earth is a subject of ongoing active debate due to the implications it has for the Earth's formation, the evolution of the early solar system and for the origin of life on Earth. In this respect, noble gases represent valuable tools due to their inertness and can thus be used as tracers of volatile sources on Earth. In this review paper, we reexamine the helium, neon, and argon data obtained for the Earth, the solar wind, lunar soils, interplanetary dust particles (IDPs), and micrometeorites. These results are discussed with a view to constraining the origin of these three noble gases on Earth and their implications for its accretion.

Helium has two stable isotopes, ^{3}He and ^{4}He. ^{3}He is primordial in the Earth's mantle but can be produced via cosmic-ray-induced spallation (cosmogenic) reactions on planetary surfaces, whereas ^{4}He is mainly radiogenic, produced in the U and Th disintegration chains. Neon has three isotopes, ^{20}Ne, ^{21}Ne, and ^{22}Ne. Its three isotopes can be produced via cosmogenic reactions but are also nucleogenic in the mantle, though the production rates for ^{20}Ne and ^{22}Ne are negligible in the Earth's mantle compared to their natural abundances (Yatsevich & Honda, 1997). Argon also has three isotopes, ^{36}Ar, ^{38}Ar, and ^{40}Ar. ^{40}Ar is the radiogenic daughter of ^{40}K, whereas ^{36}Ar and ^{38}Ar are primordial in the Earth's mantle but can also be produced via cosmogenic reactions on planetary surfaces. Therefore, the two isotopic ratios $^{20}Ne/^{22}Ne$ and $^{38}Ar/^{36}Ar$ constitute powerful tracers of volatile sources, whereas the $^{21}Ne/^{22}Ne$ ratio allows us to monitor any cosmogenic and nucleogenic components in these sources. Indeed, ^{21}Ne is a rare isotope and is thus more affected by cosmogenic and nucleogenic production, in contrast to the more abundant ^{20}Ne, ^{22}Ne, and ^{36}Ar.

Several sources for Earth's light noble gas inventory can be envisaged: (1) the implanted solar wind, (2) solar nebula gas, and (3) a cometary source and/or a chondritic component. In noble gas cosmo/geochemistry, different observed components with distinct isotopic compositions have been attributed to these sources: (1) the component "A" carried by presolar grains being found in chondrites (mostly in carbonaceous chondrites), (2) the component "B" corresponding to the implanted solar wind (Black & Pepin, 1969; Moreira,

2013; Pepin, 1967), and (3) the so-called "phase Q" (Busemann et al., 2000). Phase Q is a carbonaceous residue found in many chondrites and differentiated metorites after acid digestion, it is only a very few percent of the total mass (Busemann et al., 2000). It is a major carrier of heavy noble gases (Kr and Xe) but is depleted in light noble gases and so will not be discussed in this paper.

There is evidence for a "solar-like" neon component in the Earth's mantle (e.g., Ballentine et al., 2005; Honda et al., 1991, 1993; Moreira et al., 1995; Sarda et al., 1988, 2000; Trieloff et al., 2000). However, it is unclear how the solar nebula gas can be distinguished from the implanted solar wind (neon B) component in the mantle, as their compositions are relatively close. Different lines of reasoning have been proposed so far (e.g., Mukhopadhyay, 2012; Trieloff et al., 2000; Yokochi & Marty, 2004, detailed in section 2) and these scenarios have strong implications for early solar system dynamics. Moreover, another source of volatiles is required to explain the isotopic composition of the atmosphere. This is explained further in section 2.

The aim of this contribution is to review the existing data acquired from samples of the Earth's mantle, the solar wind, and lunar soils that record isotopic signatures of the implanted solar wind, IDPs, and micrometeorites. Having established the different isotopic composition of these potential volatile sources, they may be compared with the light noble gas signature of the Earth. In particular, we shed light on whether implanted solar wind or solar nebula gas contributed to Earth's noble gas composition. We reevaluate the isotopic and elemental compositions of the B component with lunar soils data and compare the results with the commonly used composition of Black (1972). Furthermore, we provide stronger constraints on the $^{20}Ne/^{22}Ne$ ratio of the primitive Earth's mantle to show that the actual measurements are close to the plume source ratio.

2. Three Models for Volatile Origin

In order to explain the origin of volatiles on Earth, three models can be invoked: (1) volatiles were already a part of the Earth's parent bodies, (2) volatiles were dissolved early in Earth's history into a magma ocean from a captured atmosphere with solar composition, and/or (3) volatiles were brought in a late veneer phase.

2.1. The Parent Body Model

Several studies advocated that light noble gases (He, Ne, and possibly Ar) were implanted onto the Earth's precursors at the beginning of solar system formation by solar wind irradiation. As such, light volatiles are already a part of the Earth's parent bodies (Ballentine et al., 2005; Colin et al., 2015; Kurz et al., 2009; Moreira, 2013; Moreira & Charnoz, 2016; Péron et al., 2016, 2017; Raquin & Moreira, 2009; Trieloff et al., 2000). The neon and argon isotopic compositions of implanted solar wind are different from the solar wind composition because the implantation process causes isotope fractionation (this is detailed in section 3.1.2). These implanted components were first studied by Pepin (1967) and Black and Pepin (1969), who defined the "B" component as corresponding to the implanted solar wind end-member. The similarity between the neon B component and the plume source neon composition led authors of these studies to suggest that light noble gases were implanted early in Earth's history (e.g., Ballentine et al., 2005; Raquin & Moreira, 2009; Trieloff et al., 2000). As seen in Figure 1, the Sun has higher abundances of He, Ne, and Ar compared with C1 chondrites and so solar wind implantation may be a viable mechanism to explain the origin of light noble gases on Earth. However, this scenario does not explain the neon isotopic composition of the Earth's atmosphere, which is significantly different from that of the mantle, and may not necessarily account for the origin of other volatiles such as moderately volatile elements. Furthermore, there is evidence for a late volatile delivery that will be discussed in subsequent sections (e.g., Albarède, 2009; Marty, 2012; Marty et al., 2017).

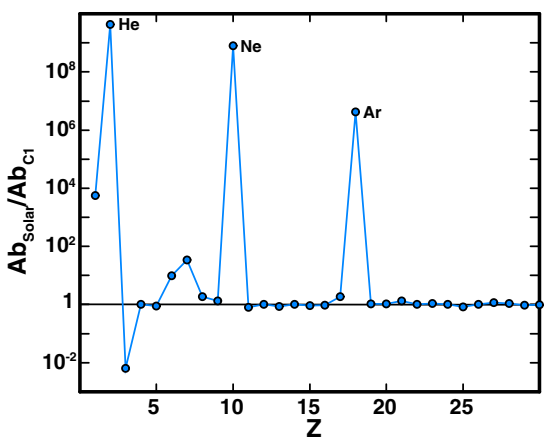

Figure 1. Solar element abundances (Ab) normalized to C1 chondrites abundances. Data are from Grevesse et al. (2005). The figure shows that the solar photosphere has higher noble gas (He, Ne, and Ar) abundances than C1 chondrites.

2.2. The Solar Nebula Gas Dissolution Model

Another model argues for direct dissolution of a primordial atmosphere to account for a fraction of Earth's volatiles (in particular noble gases). In this model, a primordial atmosphere would have been captured by gravity early in Earth's history from the solar nebula (in the first few Myr before the nebula gas was blown-off). Solar gases would have then been effectively dissolved during vigorous stirring of an early magma ocean. This scenario was proposed by Mizuno et al. (1980) who used numerical modeling to show that solar gases can be dissolved and trapped in the mantle following capture of a solar gas atmosphere. Moreover, "solar-like" $^{20}Ne/^{22}Ne$ ratios were measured in plume-derived samples (Harper & Jacobsen, 1996; Mukhopadhyay, 2012; Yokochi & Marty, 2004).

2.3. The Late Veneer Model

Geochemical and astrophysical evidence shows that a late veneer phase could have contributed to a fraction of Earth's volatiles. The late veneer, initially thought to be composed of chondritic material, was invoked to explain the highly siderophile element content of the mantle (Albarède, 2009; Drake & Righter, 2002). As chondrites are also rich in volatiles, they are also thought to have brought highly volatile elements like hydrogen and carbon (Hirschmann, 2016) in addition to moderately volatile elements such as zinc (Albarède, 2009). The material added to the Earth during this phase could either be a small fraction of comets (in particular constrained by the D/H, $^{15}N/^{14}N$, and xenon isotopic ratios) or chondritic material or a mix of both sources (e.g., Albarède, 2009; Halliday, 2013; Marty, 2012; Marty et al., 2017; Schlichting & Mukhopadhyay, 2018). Astrophysical models also support the late delivery of material coming from the outer solar system due to the inward and outward migrations of Jupiter and Saturn, scattering some asteroids or planetesimals to the terrestrial planets (e.g., Morbidelli et al., 2000; O'Brien et al., 2014; Walsh et al., 2011). The late veneer hypothesis could also account for the low $^{20}Ne/^{22}Ne$ ratio of the atmosphere compared with that of the mantle, since material from the outer solar system may have lower $^{20}Ne/^{22}Ne$ ratios (close to the Ne-A ratio) such as the carbonaceous chondrites (e.g., Mazor et al., 1970; Pepin, 1967). However, this scenario alone cannot explain the "solar-like" mantle $^{20}Ne/^{22}Ne$ ratio (sections 2.1 and 2.2) and so at least two light noble gas sources are required to explain the Earth's volatile composition. Gas loss from the Earth's atmosphere via hydrodynamic escape (Hunten et al., 1987) could also account for the present-day atmospheric neon composition, although the processes involved and the timing of this loss are unknown, and it seems even unlikely based on all the noble gases and major volatiles (H, C, and N) compositions (Schlichting & Mukhopadhyay, 2018). This latter scenario will not be discussed further in this paper.

3. Compilation of Mantle, Lunar Soils, IDPs, Micrometeorites, and Solar Wind Neon and Argon Data

To support the discussion on the three different models, we present a compilation of data from oceanic island basalts (OIB), lunar soils, IDPs, micrometeorites, and solar wind measurements.

3.1. Isotopic Compositions

3.1.1. The Plume Source Composition

In this contribution, we focus on OIB data with high $^{3}He/^{4}He$ ratios because the plume sources with high $^{3}He/^{4}He$ ratios (i.e., the lower mantle or the core-mantle boundary; Coltice et al., 2011; French & Romanowicz, 2015) may best represent a primitive noble gas reservoir (e.g., Allègre et al., 1983; Kurz et al., 1982), meaning some high $^{3}He/^{4}He$ OIBs may tap the Earth's primordial noble gas signature. In comparison, the upper mantle is known to be extensively degassed (e.g., Allègre et al., 1983; Parai & Mukhopadhyay, 2015) and it may be sensitive to atmospheric heavy noble gas recycling via subduction (Ne recycling would not be very efficient but Ar recycling could be important; Holland & Ballentine, 2006; Jackson et al., 2013; Kendrick et al., 2011; Smye et al., 2017). So the upper mantle noble gas composition likely no longer represents that of the primitive Earth. We assume the existing data on high $^{3}He/^{4}He$ OIBs best represent the plume sources but this is based on a limited number of samples.

Only a few studies present high precision neon and argon data for OIBs (Colin et al., 2015; Kurz et al., 2009; Mukhopadhyay, 2012; Péron et al., 2016, 2017; Trieloff et al., 2000; supporting information Figure S-1). Indeed, submarine or subglacial glass samples, with primitive noble gases (He and Ne), are needed for such

analyses so that the mantle gases were quenched and trapped inside the vesicles. Samples from only a few hot spots, namely Hawaii, Galápagos, and Iceland, fulfill these requirements. We do not emphasize data on OIB phenocrysts because such samples are much more prone to atmospheric contamination and also in some cases the uncertainties on isotopic ratios are high due to the low gas content (e.g., Jackson et al., 2009; Yokochi & Marty, 2004). We also do not consider the data from Pető et al. (2013) because they studied basalts from the Rochambeau rift (Lau basin), which is a more complex geologic context than OIBs rendering interpretation of noble gas data more difficult.

Trieloff et al. (2000) analyzed samples from Hawaii and Iceland by step-crushing and the highest $^{20}Ne/^{22}Ne$ ratios all cluster around 12.50 except for one that gave 12.85 ± 0.31 (1σ) from an Icelandic sample. Mukhopadhyay (2012) measured $^{20}Ne/^{22}Ne$ ratios by step-crushing samples from Iceland and obtained values as high as 12.74 ± 0.03, 12.76 ± 0.01, and 12.88 ± 0.06 (1σ). Colin et al. (2015) found a highest value of 12.73 ± 0.04 (1σ) also by step-crushing an Icelandic sample. The highest $^{20}Ne/^{22}Ne$ ratios obtained by step-crushing for the Fernandina volcano (one of the volcanoes that shows the most primitive He and Ne signatures for the Galápagos hot spot) are 12.72 ± 0.11, 12.79 ± 0.05, 12.85 ± 0.05, and 12.91 ± 0.07 (1σ) (Kurz et al., 2009; Péron et al., 2016; supporting information Figure S-1).

However, noble gases analyzed by step-crushing are susceptible to contamination by air via cracks and opened vesicles (e.g., Ballentine & Barfod, 2000), rendering the precise determination of plume mantle source-derived neon and argon isotopic ratios difficult (in supporting information Figure S-1, step-crushing data fall on a mixing line between the atmospheric and mantle end-members). In this respect, laser ablation analyses, which consist of targeting individual bubbles with a laser, constitute a very powerful alternative, as introduced by Burnard et al. (1997) and Burnard (1999) in the late 90s. Subsequently, only a few studies have used this technique due to analytical setup and blank issues (Colin et al., 2013, 2015; Péron et al., 2016, 2017; Raquin et al., 2008). Raquin et al. (2008) showed that laser ablation can effectively overcome the issue of atmospheric contamination and Colin et al. (2013) first scanned their samples via X-ray microtomography to locate the bubbles. This has proved to be an effective combination, which was then used by Colin et al. (2015) for Iceland samples and by Péron et al. (2016, 2017) for Galápagos samples.

Colin et al. (2015) derived a $^{20}Ne/^{22}Ne$ ratio of 12.7 for the Iceland mantle source with a best fit to their step-crushing and laser ablation data. For the Galápagos hot spot, Péron et al. (2017) showed that, given the similarity between all their vesicle data, it is more appropriate to consider mean isotopic ratios measured with laser ablation instead of the highest step-crushing values obtained by Péron et al. (2016) that were not reproduced. They hence suggested that the $^{20}Ne/^{22}Ne$ ratio of the Galápagos mantle source is 12.65 ± 0.04 (supporting information Figure S-1).

The latter OIBs source values are probably lower limits since mixing with the upper mantle in the mantle plume itself cannot be excluded and would decrease the $^{20}Ne/^{22}Ne$ ratio (the upper mantle $^{20}Ne/^{22}Ne$ ratio is about 12.5–12.6; e.g., Moreira, 2013). The primitive mantle $^{20}Ne/^{22}Ne$ ratio can be estimated based on the correlation of $^{21}Ne/^{22}Ne$ corrected for air contamination with $^{4}He/^{3}He$ as shown by Moreira and Allègre (1998) and Moreira (2013). Data in such a diagram can be explained by mixing between a primitive mantle and the upper mantle with a hyperbolic curvature, corresponding to the ratio $(^{3}He/^{22}Ne)_{Upper\ mantle}/(^{3}He/^{22}Ne)_{Primitive\ mantle}$, which is likely between 5 and 10 (Hopp et al., 2004; Hopp & Trieloff, 2008; Moreira, 2013; Moreira & Allègre, 1998). This also means that data in a diagram $^{20}Ne/^{22}Ne$ corrected for air contamination versus $^{4}He/^{3}He$ will also form a hyperbola with a similar curvature (laser ablation data are assumed not to be air contaminated and so do not need correction).

In the following, the diagram $^{20}Ne/^{22}Ne$ corrected for air contamination versus $^{4}He/^{3}He$ is used to present new estimates of the primitive mantle $^{20}Ne/^{22}Ne$ ratio. For this calculation, a hyperbolic equation is considered assuming that the primitive mantle $^{4}He/^{3}He$ ratio is around 15,000 (i.e., $^{3}He/^{4}He$ ratio of $50 \times Ra$ with Ra the atmospheric $^{3}He/^{4}He$ ratio; Starkey et al., 2009; Stuart et al., 2003), the Galápagos mantle source measured $^{4}He/^{3}He$ ratio is 24,085 (i.e., $30 \times Ra$; Kurz et al., 2009, 2014) and $^{20}Ne/^{22}Ne$ ratio is between 12.65 and 12.9 (this corresponds to measured values with laser ablation; Péron et al., 2016, 2017), the upper mantle $^{4}He/^{3}He$ ratio is 90,000 (i.e., $8 \times Ra$; Moreira, 2013) and $^{20}Ne/^{22}Ne$ ratio is between 12 and 12.6 (Moreira et al., 1998) for a hyperbolic curvature varying between 5 and 10 (Figure 2).

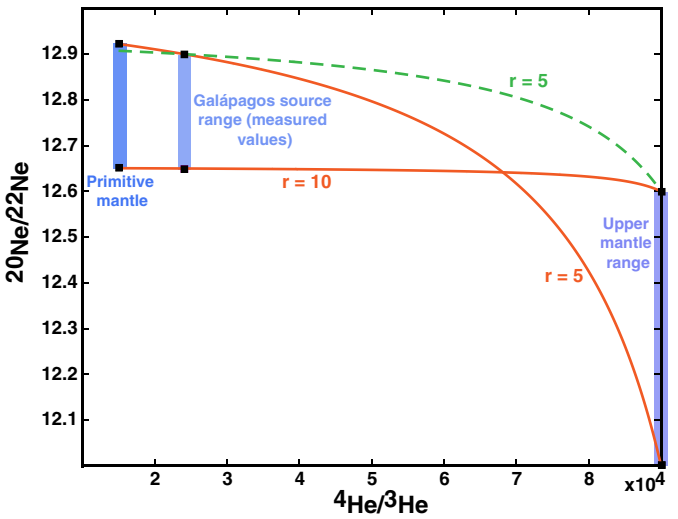

Figure 2. Mixing hyperbola between the primitive lower mantle and the upper mantle in a diagram $^{20}Ne/^{22}Ne$ corrected for shallow atmospheric contamination—$^{4}He/^{3}He$ (also refers to the corresponding figure in a diagram $^{21}Ne/^{22}Ne$ corrected for shallow atmospheric contamination—$^{4}He/^{3}He$ in Moreira (2013)). The hyperbola curvature *r* represents the ratio $(^{3}He/^{22}Ne)_{Upper\ mantle}/(^{3}He/^{22}Ne)_{Primitive\ mantle}$. The three mauve areas show the considered upper mantle, plume mantle source (Galápagos hot spot source), and the calculated primitive mantle $^{20}Ne/^{22}Ne$ ranges. The two orange curves represent the maximum and minimum values for the primitive mantle. The green dotted curve is a more realistic case with a plume mantle source $^{20}Ne/^{22}Ne$ of 12.9 (highest reasonable value). The main point is that the primitive mantle $^{20}Ne/^{22}Ne$ ratio is close to the plume mantle source measured values even with mixing with the upper mantle.

We thus determine extreme values (minimum and maximum) for the primitive mantle $^{20}Ne/^{22}Ne$ ratio. Indeed, this calculation takes into account a large range of possible values for the upper mantle and Galápagos mantle source $^{20}Ne/^{22}Ne$ ratios and for the hyperbolic curvature.

The mantle $^{3}He/^{22}Ne$ ratio is not known precisely. It is between 5 and 10 for the upper mantle (Moreira et al., 1998; Tucker & Mukhopadhyay, 2014) and around 2 for the Galápagos and Iceland mantle sources (e.g., Kurz et al., 2009; Moreira & Kurz, 2013; Mukhopadhyay, 2012; Péron et al., 2016, 2017; Tucker & Mukhopadhyay, 2014). It seems even lower for samples from West Greenland, assumed to represent the protoicelandic plume (Graham et al., 1998). Indeed, we present new data obtained by crushing olivine melt inclusions of two samples from the Svartenhuk Halvø Peninsula, West Greenland coast (Baffin Bay; Table 1 and supporting information text S1). This gives a $^{3}He/^{22}Ne$ ratio of around 0.85 when extrapolating data of Table 1 to a $^{20}Ne/^{22}Ne$ of 12.7. Considering that these samples also define mixing lines between the plume source and the upper mantle, it is likely that the plume source $^{3}He/^{22}Ne$ ratio is lower than 0.85. Assuming that the $^{3}He/^{22}Ne$ ratio is 5 for the upper mantle (Moreira et al., 1998) and 1 for the plume mantle source, this gives a curvature of 5 in the most extreme case.

Figure 2 shows the acceptable range of values for the primitive mantle $^{20}Ne/^{22}Ne$ ratio, which is between 12.65 and 12.92 based on the input parameters (that is the $^{3}He/^{4}He$ ratios of the primitive mantle, Galápagos source and upper mantle, the $^{20}Ne/^{22}Ne$ ratios of the upper mantle and Galápagos source, and the $^{3}He/^{22}Ne$ ratios that define the curvature). The most important observation in this figure is that the $^{20}Ne/^{22}Ne$ ratio does not vary significantly between the Galápagos source and the primitive mantle. Even in the most extreme case, that is with a hyperbolic curvature of 5, a plume (Galápagos) mantle source $^{20}Ne/^{22}Ne$ ratio of 12.9 (highest measured value) and an upper mantle $^{20}Ne/^{22}Ne$ of 12 (likely to be a lower limit), the primitive mantle $^{20}Ne/^{22}Ne$ ratio is up to 12.92. This suggests that actual OIB $^{20}Ne/^{22}Ne$ measurements are likely very close to the primitive mantle value and that mixing with the upper mantle does not change significantly the $^{20}Ne/^{22}Ne$ ratio.

The $^{38}Ar/^{36}Ar$ ratio measured in OIB glass samples is very close to the atmospheric ratio (supporting information Figure S-2; Mukhopadhyay, 2012; Péron et al., 2017; Trieloff et al., 2000), as also discussed by Raquin and Moreira (2009) even if their corresponding $^{20}Ne/^{22}Ne$ ratios are lower than those measured in the other studies (Mukhopadhyay, 2012; Péron et al., 2017; Trieloff et al., 2000).

3.1.2. Lunar Soil Composition

The Moon's surface is exposed to the solar wind and to galactic cosmic rays (GCRs). The noble gas composition of lunar soils was extensively studied, in particular to determine the noble gas composition of the solar wind, from samples returned from the Apollo and Luna missions in the seventies (e.g., Benkert et al., 1993; Bogard et al., 1973; Eberhardt et al., 1970, 1972; Füri et al., 2014; Heymann & Yaniv, 1970; Hübner et al., 1975; Mortimer et al., 2016; Pepin et al., 1999, 1970). Pepin (1967) and Black and Pepin (1969) were among

Table 1
He and Ne Elemental and Isotopic Compositions Measured on Olivine Melt Inclusions of Two Samples From the Svartenhuk Halvø Peninsula, West Greenland Coast (Baffin Bay)

Samples	*m* (g)	^{4}He ($\times10^{-9}$ cm^3 STP/g)	*s*	$^{3}He/^{4}He$ ($\times$Ra)	*s*	^{22}Ne ($\times10^{-13}$ cm^3 STP/g)	*s*	$^{20}Ne/^{22}Ne$	*s*	$^{21}Ne/^{22}Ne$	*s*
S35E7	0.570	8.20	0.96	34.89	0.83	8.06	0.29	11.47	0.12	0.0323	0.0015
S33E7	0.0719	6.44	0.96	31.04	2.37	14.8	0.3	10.29	0.22	0.0292	0.0032

Note. Uncertainties are 1σ. Details about the method can be found in supporting information Text S1.

the first, studying gas-rich meteorites, to define the B component, which would correspond to implanted solar wind and whose isotopic composition was found to be $^{20}Ne/^{22}Ne = 12.52 \pm 0.18$ and $^{38}Ar/^{36}Ar$ ratio $= 0.1862 \pm 0.0042$ (Black, 1972).

The implanted solar wind, sampled in lunar soils, does not have the same composition as the solar wind, because implantation fractionates the isotopes (Grimberg et al., 2006). Solar wind ions have the same escape speed but different kinetic energies due to their different masses, causing the heaviest ions to be implanted deeper into grains. This implantation process also removes grain surfaces (a sputtering effect), enriched in light isotopes, which leads to complementary heavy isotope enrichment in the residual grains compared with the composition of the solar wind (Raquin & Moreira, 2009). Solar wind implantation is a surface effect as it affects the first few hundred nanometers of grains (Grimberg et al., 2006).

The implanted solar wind composition was also calculated via numerical modeling ($^{20}Ne/^{22}Ne \sim 12.7$; Moreira, 2013; Moreira & Charnoz, 2016; Raquin & Moreira, 2009). Black (1972)'s estimate is lower but still consistent within the uncertainties. Moreira and Charnoz (2016) also show that a grain population may have a higher $^{20}Ne/^{22}Ne$ ratio if the implantation/sputtering process does not reach a steady state (e.g., for a few kyr) but this is not the case for the Moon surface.

The composition suggested by Black (1972), even if uncertainties are large, is very often considered as the reference but is now challenged by these recent numerical models. The B component composition is critical to terrestrial studies since similar isotopic compositions are measured for some plume mantle sources (section 2.1). In this paper, we reevaluate the B component neon and argon isotopic ratios from lunar soil data.

We consider only data from lunar soils, breccias, fines, and ilmenites (a mineral with a high tendency to retain noble gases; Eberhardt et al., 1970), i.e., samples that constitute or have constituted the lunar regolith (McKay et al., 1991) and have been exposed to solar wind irradiation for thousands of years. These samples are hence expected to contain a large fraction of noble gases from solar wind implantation, contrary to lunar rocks (e.g., Füri et al., 2015; Mortimer et al., 2015) that are not taken into account. If the data were acquired with step-etching or step-heating, we consider the total composition and not each step individually. Indeed, to define the B component composition, these techniques cannot be used, because, in the first few steps, only gases from the outer layers of the sample are released and are enriched in light isotopes. As etching progresses, gases are liberated from deeper layers enriched in heavier isotopes (Grimberg et al., 2006). Step-etching measurements led to the identification of a so-called SEP component (solar-energetic particles), which is no longer considered as a component, but as an analytical artifact (Grimberg et al., 2006; Wieler et al., 2007).

Data from the following studies are used: Eberhardt et al. (1970), Funkhouser et al. (1970), Heymann and Yaniv (1970), Hintenberger et al. (1970), Kirsten et al. (1970) (only grains that were not etched), Pepin et al. (1970), Yaniv and Heymann (1971), Eberhardt et al. (1972), Heymann et al. (1972), Bogard et al. (1973), Eugster et al. (1973), Heymann et al. (1973), Kirsten et al. (1973) Bogard et al. (1974), Jordan et al. (1974), Bogard and Hirsch (1975), Hübner et al. (1975), Eugster (1985), Benkert et al. (1993), Rider et al. (1995), and Pepin et al. (1999).

We also report these data relative to the air standard ($^{20}Ne/^{22}Ne = 9.80$, $^{21}Ne/^{22}Ne = 0.029$, and $^{38}Ar/^{36}Ar = 0.1880$) in case the authors used different values. The standard isotopic compositions in these studies were not always mentioned, and this may contribute to the data scatter.

The lunar soils data are represented in a three Ne isotope diagram in Figure 3. The vast majority have a $^{20}Ne/^{22}Ne$ ratio between 12 and 13.50; some data fall on a mixing line between the cosmogenic ($^{21}Ne/^{22}Ne = 0.8–1$; Wieler, 2002) and Ne-B end-members. In order to overcome the cosmogenic effect, we first select only the data for which $^{21}Ne/^{22}Ne$ is lower than 0.05, which seems an appropriate limit (Figure 3). Then we use the same statistical method as Péron et al. (2017) to calculate the Ne-B $^{20}Ne/^{22}Ne$ ratio, that is, we consider a Gaussian distribution for each datum and then sum these distributions for a given isotopic ratio to obtain a global curve. With this technique, data from Yaniv and Heymann (1971) and Heymann et al. (1972) are excluded because no uncertainties on isotopic ratios were reported.

Supporting information Figure S-3 shows the global curve for the $^{20}Ne/^{22}Ne$ ratio. A main peak can be observed, which probably correspond to the steady state Ne-B ratio. The numerous secondary peaks observed are attributed to data scatter rather than real noble gas components. Indeed, as mentioned earlier, data scatter may result from adopting different standard values, or the diversity of grain sizes analyzed.

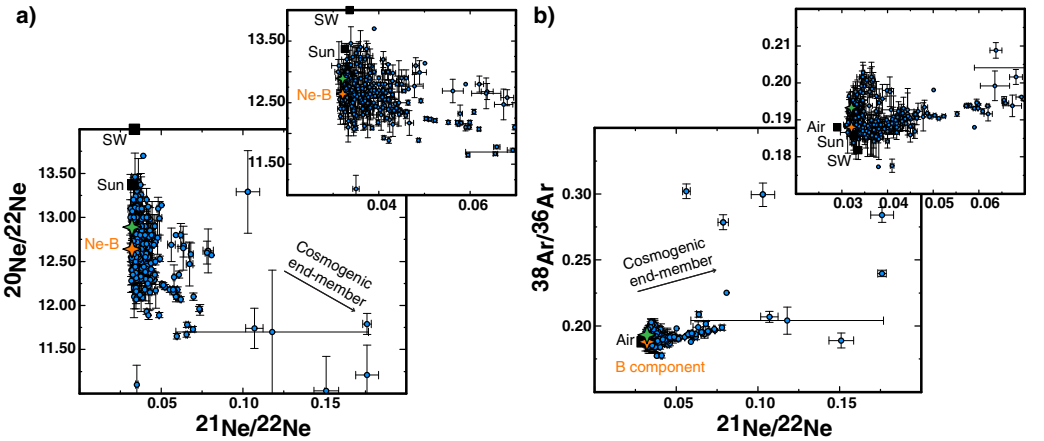

Figure 3. Lunar soils data in (a) a three neon isotope plot and (b) a diagram $^{38}Ar/^{36}Ar$-$^{21}Ne/^{22}Ne$. Data are from Eberhardt et al. (1970), Funkhouser et al. (1970), Heymann and Yaniv (1970), Hintenberger et al. (1970), Kirsten et al. (1970), Pepin et al. (1970), Yaniv and Heymann (1971), Eberhardt et al. (1972), Heymann et al. (1972), Bogard et al. (1973), Eugster et al. (1973), Heymann et al. (1973), Kirsten et al. (1973), Bogard et al. (1974), Jordan et al. (1974), Bogard and Hirsch (1975), Hübner et al. (1975), Eugster (1985), Benkert et al. (1993), Rider et al. (1995), and Pepin et al. (1999). Solar wind (SW; Pepin et al., 2012) and Sun (Heber et al., 2012). The orange star corresponds to the calculated B component composition from all the data and the green star to the B component composition from ilmenites only (see text).

Ilmenites have systematically higher $^{20}Ne/^{22}Ne$ ratios (around 13) because they are less affected by diffusive noble gas loss (so they lose less ^{20}Ne, located preferentially at the surface of the grains; e.g., Eberhardt et al., 1970). The main peak in supporting information Figure S-3 is thus fitted and we determine a value of 12.64 ± 0.08 (1σ) for the B component $^{20}Ne/^{22}Ne$ ratio. The latter uncertainty 0.08 (1σ) is derived mathematically but may be too low as we insist just above that lunar soils compositions seem to depend on grain sizes and compositions.

We also check that a $^{21}Ne/^{22}Ne$ ratio of 0.05 is a consistent limit by using other values for this ratio (0.035, 0.040, and 0.045). Similar results are obtained, but a value of 0.035 seems too restrictive (Figure 3).

For the $^{21}Ne/^{22}Ne$ ratio of Ne-B, we take the value of 0.0321 ± 0.0002 calculated by Raquin and Moreira (2009) from Pepin et al. (2012)'s solar wind value. It is inadvisable to use data for lunar soils since ^{21}Ne is very sensitive to cosmogenic production.

For the $^{38}Ar/^{36}Ar$ ratio represented in Figure 3, we process the data in the same way as for the $^{20}Ne/^{22}Ne$ ratio. The global and fitted curves are shown in supporting information Figure S-4. The fit gives a value of 0.1878 ± 0.0008 (1σ), which corresponds to the atmospheric ratio. As for neon, a similar result is obtained for different data filtering with lower $^{21}Ne/^{22}Ne$ ratios. The samples are unlikely contaminated by air because their $^{40}Ar/^{36}Ar$ ratios are between 1 and 5 for nearly all of them, whereas the atmospheric ratio is 298.6 (Lee et al., 2006).

The Gaussian method seems consistent as removing some data randomly does not affect the results for the two isotopic ratios $^{20}Ne/^{22}Ne$ and $^{38}Ar/^{36}Ar$. We compare these results with those obtained via the following method. We consider that the data are the result of mixing between a cosmogenic and a "B" end-member and fitted them in a R-$^{21}Ne/^{22}Ne$ diagram (with R either the $^{20}Ne/^{22}Ne$ ratio or $^{38}Ar/^{36}Ar$ ratio). For this exercise, we use the cosmogenic isotopic composition of Wieler (2002) ($^{20}Ne/^{22}Ne \sim 0.9$, $^{21}Ne/^{22}Ne = 0.8$–1 and $^{38}Ar/^{36}Ar \sim 1.59$) and we adjusted a hyperbola to find the $^{20}Ne/^{22}Ne$ and $^{38}Ar/^{36}Ar$ ratios of the B component as well as the hyperbolic curvature r (for the $^{20}Ne/^{22}Ne$ ratio, $r = 1$). The result is the same for the $^{38}Ar/^{36}Ar$ ratio and for the $^{20}Ne/^{22}Ne$ ratio we find a value of 12.72 ± 0.02 (1σ), which is close to the value of 12.64 ± 0.08. But the cosmogenic $^{20}Ne/^{22}Ne$ ratio is poorly known (Wieler, 2002) and so the latter method may not be suitable in this case.

By comparison, the Gaussian method applied only to ilmenites data (37 samples from Benkert et al., 1993; Eberhardt et al., 1970, 1972; Pepin et al., 1999) yields a $^{20}Ne/^{22}Ne$ ratio of 12.89 ± 0.15 (1σ) and a $^{38}Ar/^{36}Ar$ ratio of 0.1933 ± 0.0024 (1σ).

Table 2
^{22}Ne and ^{36}Ar Concentrations in mol/g for the Earth, Lunar Soils, IDPs, and Micrometeorites

	^{22}Ne (mol/g)	^{36}Ar (mol/g)
Lunar soils (section 3.1.2)	6×10^{-11} to 2×10^{-7}	9×10^{-11} to 8×10^{-8}
IDPs-micrometeorites	4.5×10^{-13} to 1.3×10^{-6}	4.5×10^{-12} to 9×10^{-8}
Bulk mantle[a]	5.8×10^{-15}	7.8×10^{-14}
Atmosphere[a]	2.27×10^{-14}	9.58×10^{-13}

[a]Concentrations are from Marty (2012).

It is important to keep in mind that lunar soils are very rich in noble gases compared to the Earth, containing between 6×10^{-11} and 2×10^{-7} mol/g of ^{22}Ne and between 9×10^{-11} and 8×10^{-8} mol/g of ^{36}Ar (Table 2 for comparison).

3.1.3. IDPs and Micrometeorites Composition

IDPs and micrometeorites are also exposed to solar wind irradiation during their transport in the solar system and may also reflect the implanted solar wind composition. Several studies report the noble gas isotopic compositions of IDPs (Hudson et al., 1981; Kehm et al., 2006; Nier & Schlutter, 1990, 1992; Pepin et al., 2000, 2001) and of micrometeorites (Bajo et al., 2012; Marty et al., 2005; Okazaki et al., 2015; Osawa et al., 2000, 2003; Osawa & Nagao, 2002a, 2002b). However, the uncertainties on the neon and argon data are big and these particles have lost a fraction of their noble gases due to heating in the Earth's atmosphere (Bajo et al., 2012; Füri et al., 2013; Kehm et al., 2006; Marty et al., 2005; Okazaki et al., 2015; Osawa et al., 2003).

Some studies tried to define the extent of atmospheric heating for their samples (Bajo et al., 2012; Kehm et al., 2006; Okazaki et al., 2015). Kehm et al. (2006) even determined a heating index from 1 to 3 based on the He and Zn contents. To compare with the heating degree mentioned by Bajo et al. (2012) estimated according to mineral composition and that of Okazaki et al. (2015) determined by the solar ^{4}He release pattern, we attribute a value of 1 for *weak* or *least* heating, a value of 1.5 for *weak to moderate* heating, a value of 2 for *moderate* heating and a value of 3 for *severe* heating, as described by Bajo et al. (2012) and Okazaki et al. (2015). For the samples studied by Marty et al. (2005), we attribute a value of 1 for the *crystalline samples*, a value of 1.5 for *scoria/crystalline samples*, a value of 2 for *scoria samples*, of 2.5 for *scoria/cosmic spherule samples*, and of 3 for *cosmic spherules*. In supporting information Figure S-5, it seems there is a slight trend showing the ^{22}Ne concentration decreasing as the heating index increases. Similar trends are observed with ^{4}He and ^{36}Ar concentrations.

In Figure 4, the ^{20}Ne/^{22}Ne ratio is represented according to the heating index (only for studies that defined a heating degree, cf., above and supporting information Figure S-5) and the ^{22}Ne concentration. The ^{20}Ne/^{22}Ne ratios are between 10 and 13. Hence, IDPs and micrometeorites have ^{20}Ne/^{22}Ne ratios close to the lunar soil ratios. But, as already mentioned, the uncertainties are big. Future studies are required to improve the precision and determine whether atmospheric entry heating modifies the noble gas isotopic ratios or not.

For the ^{38}Ar/^{36}Ar ratio, the IDPs and micrometeorites compositions are also near the lunar soil composition, though an exact determination is prevented due to the big uncertainties.

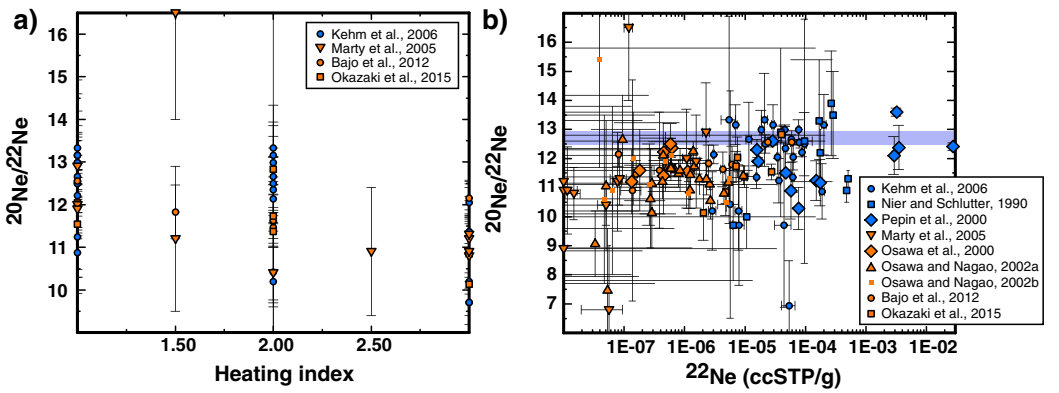

Figure 4. ^{20}Ne/^{22}Ne versus (a) the heating index and (b) the ^{22}Ne content for some IDPs (Kehm et al., 2006) and micrometeorites (Bajo et al., 2012; Marty et al., 2005; Okazaki et al., 2015). Bajo et al. (2012), Okazaki et al. (2015), and Marty et al. (2005) only characterized the heating degree of their samples and we then attributed a heating index between 1 and 3 to compare with the index of Kehm et al. (2006) (see text and also supporting information Figure S-5). IDPs are in blue and micrometeorites in orange. The mauve area in Figure 4b shows the Ne-B composition. The ^{20}Ne/^{22}Ne ratio seems to decrease as the heating degree increases and so as the ^{22}Ne content decreases, even if uncertainties are very large.

Table 3
Solar Wind Neon and Argon Isotopic Composition Determined on Genesis Collectors by Several Authors

	$^{20}Ne/^{22}Ne$	s	$^{21}Ne/^{22}Ne$	s	$^{38}Ar/^{36}Ar$	s
Meshik et al. (2007)	13.97	0.03	0.0346	0.0003	0.1818	0.0002
Grimberg et al. (2008)[a,b]	13.81	0.12	0.0330	0.0002	0.1880	0.0023
	13.75	0.09	0.0330	0.0005		
Heber et al. (2009)	13.78	0.03	0.0332	0.0001	0.1823	0.0003
Vogel et al. (2011)					0.1813	0.0003
Pepin et al. (2012)	14.00	0.04	0.0336	0.0002	0.1818	0.0005
Meshik et al. (2014)[c]					0.1814	0.0004

Note. The stated uncertainties correspond to 1σ. The isotopic composition is indicated relative to air isotopic ratios $^{20}Ne/^{22}Ne = 9.80$, $^{21}Ne/^{22}Ne = 0.029$, and $^{38}Ar/^{36}Ar = 0.1880$.
[a]No standard atmospheric neon isotopic composition was provided. [b]The first value is from CSSE experiment and the second from total extraction. [c]The value determined on the PAC collector is indicated.

It is important to note that IDPs and micrometeorites are very rich in noble gases as they can contain up to 1.3×10^{-6} mol/g of ^{22}Ne (Figure 4). Even the particles with the lowest ^{22}Ne concentrations (around 4.5×10^{-13} mol/g, Figure 4) are very rich compared to the Earth bulk mantle and the Earth atmosphere (Table 2). For ^{36}Ar, IDPs and micrometeorites can contain from 4.5×10^{-12} to 9×10^{-8} mol/g (Table 2).

3.1.4. Solar Wind Composition

The solar wind composition was first estimated with the solar wind composition experiment, which was established during Apollo missions 11, 12, 14, 15, and 16 (Geiss et al., 2004 for a review). Recently, the neon and argon solar wind composition was reevaluated more precisely thanks to the Genesis mission (Grimberg et al., 2008; Heber et al., 2009; Meshik et al., 2012, 2014, 2007; Pepin et al., 2012; Vogel et al., 2011).

The results obtained on different Genesis collector types are summarized in Table 3. The $^{20}Ne/^{22}Ne$ ratios agree well with one another within uncertainties and vary between 13.75 and 14.00 (Grimberg et al., 2008; Heber et al., 2009; Meshik et al., 2007; Pepin et al., 2012). As for the $^{21}Ne/^{22}Ne$ ratio, the solar wind value lies between 0.0330 and 0.0336. The value of 0.0346 from Meshik et al. (2007) therefore appears to be too high. Indeed, the authors indicate that they are not confident in this value due to uncertainty in the $^{20}NeH^{+}$ corrections applied on the $^{21}Ne^{+}$ signal. The $^{38}Ar/^{36}Ar$ ratio varies between 0.1814 and 0.1823. In light of these values, the value of 0.1880 from Grimberg et al. (2008) also seems too high. The authors mention that the

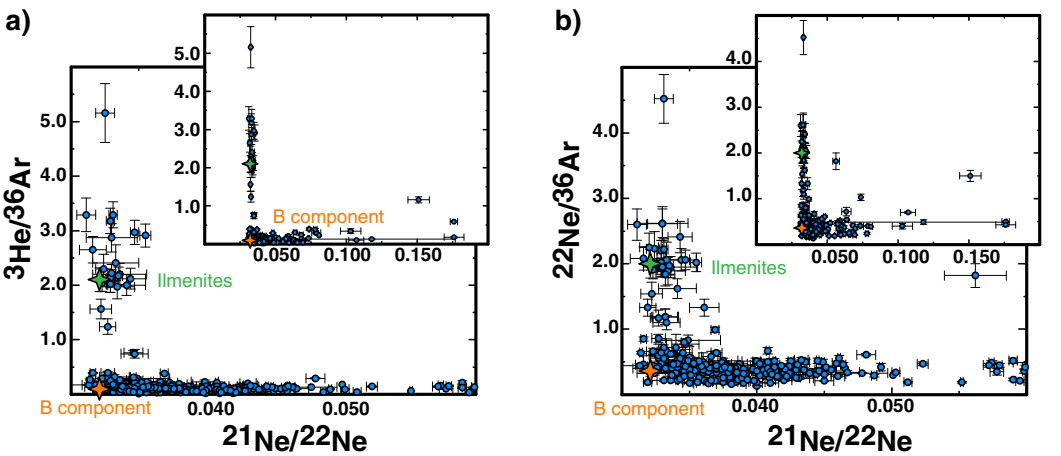

Figure 5. Elemental ratio (a) $^{3}He/^{36}Ar$ and (b) $^{22}Ne/^{36}Ar$ versus $^{21}Ne/^{22}Ne$ for lunar soils data, ilmenites have higher $^{3}He/^{36}Ar$ ratio (~2.0–3.0) and $^{22}Ne/^{36}Ar$ ratio (~2.0). Data are from Eberhardt et al. (1970), Funkhouser et al. (1970), Heymann and Yaniv (1970), Hintenberger et al. (1970), Kirsten et al. (1970), Pepin et al. (1970), Yaniv and Heymann (1971), Eberhardt et al. (1972), Heymann et al. (1972), Bogard et al. (1973), Eugster et al. (1973), Heymann et al. (1973), Kirsten et al. (1973), Bogard et al. (1974), Jordan et al. (1974), Bogard and Hirsch (1975), Hübner et al. (1975), Eugster (1985), Benkert et al. (1993), and Rider et al. (1995). The orange star corresponds to the calculated B component composition from all the data and the green star to the B component composition from ilmenites only (see text).

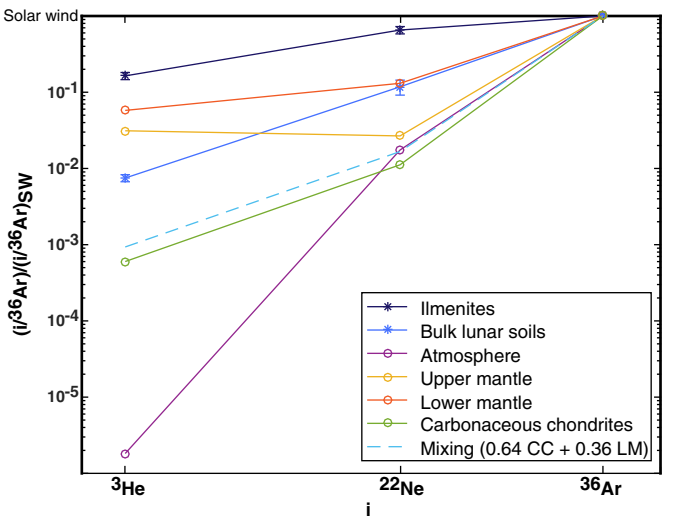

Figure 6. Elemental ratios of the solar-wind-implanted component (B component) determined for the bulk lunar soils (light blue curve) and also only with ilmenites (dark blue curve). The elemental ratios are normalized to the Heber et al. (2009)'s solar wind values. By comparison, the atmosphere, the upper mantle (Moreira et al., 1998), the lower mantle (Péron et al., 2017), the carbonaceous chondrites (Mazor et al., 1970) compositions are indicated. The light blue dotted line represents a mixing with 64% of carbonaceous chondrites (CC) and 36% of gases from the lower mantle (LM, at least the plume source reservoir), which allows us to reproduce the atmospheric $^{22}Ne/^{36}Ar$ (see section 4.4 for details).

argon blank corrections were often high and their $^{40}Ar/^{36}Ar$ ratios are sometimes close to the air ratio, likely indicating variable atmospheric contamination.

Heber et al. (2012) have estimated the solar isotopic composition using a correlation approach ($^{20}Ne/^{22}Ne = 13.36 \pm 0.09$ and $^{38}Ar/^{36}Ar = 0.1857 \pm 0.0010$ [relative to $^{38}Ar/^{36}Ar_{air} = 0.1880$]).

3.2. Elemental Compositions

In order to evaluate the potential sources that delivered Earth's volatiles, it is also important to consider the elemental compositions of the different potential sources mentioned above. We first determine a mean elemental composition for the lunar soils (that is for the B component) using the data presented in section 3.1.2, applying the Gaussian approach (Figures 5 and 6 and supporting information Figure S-6). Since bulk lunar soils may not be appropriate for determining elemental compositions due to diffusive loss of noble gas (in particular helium loss; Eberhardt et al., 1970), we also calculate the ilmenite noble gas elemental composition (Figure 6).

All the results in Figure 6 are normalized to Heber et al. (2009)'s solar wind elemental ratios. The differences for the two elemental ratios $^{3}He/^{36}Ar$ and $^{22}Ne/^{36}Ar$ between the studies of Meshik et al. (2007), Heber et al. (2009), and Pepin et al. (2012) are not discussed here and are beyond the scope of this study.

Results for the B component differ significantly, depending on whether bulk lunar soils or ilmenites are considered, with a $^{3}He/^{36}Ar$ ratio of 0.10 ± 0.01 and 2.1 ± 0.22 (1σ), respectively, and a $^{22}Ne/^{36}Ar$ ratio of 0.36 ± 0.08 and 2.00 ± 0.22 (1σ), respectively (Table 4). The bulk lunar soils clearly show helium and neon losses (Figure 6). It is interesting to note that ilmenites have a $^{3}He/^{22}Ne$ ratio close to 1, which is similar to that of OIBs (section 3.1.1).

4. Discussion

4.1. The Earth Composition

Table 4 shows a summary of the isotopic and elemental compositions discussed in section 3.

The similarity between the Earth's mantle and the B component $^{20}Ne/^{22}Ne$ ratio is striking (section 3 and supporting information Figures S-1 and S-2 and Figure 3). Measured values for the plume mantle sources

Table 4
*Summary of Neon and Argon Isotopic and Elemental Compositions for the Galápagos Mantle Source (*Péron et al., 2017*), Lunar Soils (Section* 3.1.3*), the Sun (*Heber et al., 2012*), Solar Wind (Sections* 3.1.4 *and* 3.2*), Solar Wind Used for Normalization in* Figure 6 *(*Heber et al., 2009*), and Carbonaceous Chondrites (*Mazor et al., 1970*) Used in* Figure 6

	$^{20}Ne/^{22}Ne$	s	$^{38}Ar/^{36}Ar$	s	$^{3}He/^{36}Ar$	s	$^{22}Ne/^{36}Ar$	s
Lower mantle	12.65	0.04	0.1887	0.0006	0.74		0.37–0.44	
Bulk lunar soils	12.64	0.08	0.1878	0.0008	0.10	0.01	0.36	0.08
Ilmenites	12.89	0.15	0.1933	0.0024	2.10	0.22	2.00	0.22
Sun	13.36	0.09	0.1857	0.0010				
Solar wind	13.75–14.00		0.1814–0.1823		9.56–12.81		3.06–4.22	
Solar wind (Heber et al., 2009)	13.78	0.03	0.1828	0.0003	12.81	0.28	3.06	0.02
Carbonaceous chondrites	8.20	0.40	0.1842	0.0044	0.0077		0.034	
Atmosphere	9.80		0.1880		2.33×10^{-5}		0.053	
Mixing (0.64 CC + 0.36 LM)	9.8				0.012		0.051	

Note. The result of the calculation mixing 64% of gases from carbonaceous chondrites with 36% of gases from the lower mantle is indicated. The isotopic compositions are indicated relative to air isotopic ratios $^{20}Ne/^{22}Ne = 9.80$, $^{21}Ne/^{22}Ne = 0.029$, and $^{38}Ar/^{36}Ar = 0.1880$.

(Galápagos, Iceland, and Hawaii) $^{20}Ne/^{22}Ne$ ratio range between 12.6 and 12.9, while the B component $^{20}Ne/^{22}Ne$ ratio is between 12.65 (bulk soils) and 12.9 (ilmenites). By contrast, the atmospheric $^{20}Ne/^{22}Ne$ ratio is very different (9.8). However, the Earth's mantle has a $^{38}Ar/^{36}Ar$ ratio indistinguishable from that of air (0.1880). The mantle $^{38}Ar/^{36}Ar$ ratio is close to the B component, as determined from bulk lunar soils. However, if one considers ilmenite only to characterize the B component, then the mantle value is significantly lower.

It is important to note that the Earth's neon and argon isotopic ratios diverge markedly from the solar wind and solar ratios (section 3 and supporting information Figures S-1 and S-2 and Figure 3).

Finally, the solar wind and the B component (ilmenites) have higher abundances of helium and neon compared with the Earth's mantle (Figure 6).

4.2. The Solar Nebula Gas Dissolution Model

As discussed in the prior sections, Earth's neon and argon composition is different from the solar wind and solar compositions. If light noble gases originated from dissolution of the solar nebula gas into an early magma ocean, this would imply that secondary processes have changed the mantle noble gas composition.

Atmospheric neon subduction would be required in such a scenario to lower the $^{20}Ne/^{22}Ne$ ratio from solar-day to the present-day mantle value. But neon recycling via subduction into the lower mantle seems rather unlikely (Holland & Ballentine, 2006; Moreira et al., 2003; Staudacher & Allègre, 1988). On the contrary, recycling of heavy noble gases including Ar could be more effective (Smye et al., 2017). It can also be argued that the plume mantle sources have a solar $^{20}Ne/^{22}Ne$ ratio and that atmospheric contamination of the samples masks the primary solar isotopic signature. But results from laser ablation analyses suggest the noble gases have been unaffected by atmospheric contamination (Colin et al., 2013, 2015; Péron et al., 2016, 2017; Raquin et al., 2008) provided that magma was not contaminated before eruption. Indeed, laser ablation analyses can only overcome the atmospheric contamination issue if this is a posteruptive process (e.g., air that fill cracks and opened vesicles after recovery on the seafloor). Magma can also be contaminated by assimilation of altered crust (e.g., Stroncik & Niedermann, 2016). The two Galápagos samples, AHA-NEMO2-D22A and AHA-NEMO2-D22B, used in the studies of Péron et al. (2016, 2017) have Cl/K ratios of 0.054 and 0.039, respectively (calculated from the data of Peterson et al., 2017), and are thus unlikely contaminated because these Cl/K ratios correspond to values for uncontaminated sources (0.01–0.08; Michael & Cornell, 1998; Peterson et al., 2017; Shimizu et al., 2016; Stroncik & Haase, 2004).

Therefore, mantle regions with solar Ne have not yet been observed and the existence of solar neon in the mantle seems unlikely.

Dissolution of solar nebula gas into a magma ocean would have had to have occurred very early in Earth's history, during the embryonic stage of planetary formation, because the nebula is blown away in a few Myr (Beckwith & Sargent, 1996; Wyatt et al., 2003). Jaupart et al. (2017) posited the possibility that dissolution of solar gases is too inefficient at the embryo stage and could not account for the Earth's neon budget. Indeed, for their numerical simulations, they considered smaller embryos (0.1–0.2 M_{Earth}) than usually assumed (0.5–1 M_{Earth}), because planetary formation models show that planetary embryos are still relatively small ($<$0.1–0.2 M_{Earth}) when the solar nebula gas is present (i.e., when noble gas dissolution could be effective; Jaupart et al., 2017).

All these arguments seem to rule out the solar nebula gas dissolution as the main light noble gas source for the Earth even if a small (negligible) contribution from solar gas cannot be excluded.

4.3. The Solar Wind Irradiation Model

As shown in section 3 and highlighted in section 4.1, the Earth $^{20}Ne/^{22}Ne$ and $^{38}Ar/^{36}Ar$ ratios are close to the B component ratios, resulting from solar wind implantation and sputtering. The identity of samples that are most representative of the B component, and can thus be compared to the Earth, remains an outstanding question. Indeed, the bulk lunar soils suffer helium and neon loss via diffusion, whereas ilmenites tend to retain their primary noble gas signatures (e.g., Eberhardt et al., 1970). These two types of samples accordingly have different neon and argon isotopic and elemental compositions. Of course, the material that accreted to form the Earth cannot have been composed solely of ilmenite. Micrometer-sized dust grains

accreted quickly, certainly faster than the duration for which lunar soils are exposed to solar wind irradiation. As a result, these primitive grains would not have suffered significant gas loss, as observed for bulk lunar soils.

Given the similarity of plume mantle and B component compositions, it is likely that a large fraction of mantle light noble gases originate from solar wind implantation at the beginning of solar system formation. But it is difficult, if not impossible, to know precisely the resulting noble gas composition of Earth precursor grains following implantation. The latter composition depends on possible gas loss, and on whether equilibrium was achieved, which is itself proportional to the irradiation time. For example, Moreira and Charnoz (2016) showed that a population of grains can have high $^{20}Ne/^{22}Ne$ ratios, up to 12.9 or more if the implantation and sputtering do not reach a steady state because a grain is not exposed to the solar wind during its entire existence. In this respect, the compositions given in sections 3.1.2 and 3.2 for bulk lunar soils and ilmenites must be regarded as approximations for the B component rather than definite compositions.

Solar wind implantation may also account for a fraction of the Earth's mantle water budget, since Bradley et al. (2014) showed that solar wind implantation on IDP grains induce the formation of a rim with vesicles containing detectable amounts of water. Water adsorption onto grains was also shown experimentally (Djouadi et al., 2011) and via modeling and density functional theory calculations (Asaduzzaman et al., 2013, 2015; Drake, 2005).

The second issue is how this solar-wind-implanted signature is preserved throughout accretion despite heating. Indeed, a fraction of solar-wind-implanted noble gases are probably lost during accretion. However, as shown in Figure 1, the solar wind has higher helium, neon and argon abundances than chondrites. Furthermore, as detailed in section 3.1.3, lunar soils, IDPs, and micrometeorites are more abundant in noble gases (by several orders of magnitude) compared to the Earth (Table 2). Therefore, only a small fraction of implanted noble gases from similar particles (a few percent of Earth's mass) is needed to account for the Earth's budget of light noble gases. Different classes of meteorites exhibit the B component signature (e.g., Black, 1970, 1971, 1972; Black & Pepin, 1969; Mazor et al., 1970; Moreira, 2013; Patzer & Schultz, 2002; Pepin, 1967), which could favor retention of this signature during accretion. A possible caveat is that these meteorites may have been extracted from regoliths and meaning they could have acquired their B component postaccretion. Further work is required to resolve this issue.

There is isotopic evidence from several elements that the Earth and enstatite chondrites are very similar (O, Ca, Ti, Cr, Ni, and Mo; e.g., Dauphas et al., 2014; Javoy, 1995; Javoy et al., 2010; Trinquier et al., 2007; Warren, 2011). The implication being that the Earth and enstatite chondrites likely form from a similar reservoir in the inner part of the disk between 0 and 1.5 AU (Dauphas et al., 2014). Moreira and Charnoz (2016) showed that the upper layers of the protoplanetary disk could be irradiated by the early Sun up to 1.5–2 AU and to 1 AU for the disk midplane. Hence, the inner disk reservoir, from which enstatite chondrites, the Earth and other terrestrial planets originate, occurred in a region of the protoplanetary disk susceptible to irradiation by the solar wind. Irradiation could occur even if the solar nebula was still present, as Moreira and Charnoz (2016) calculated that the mean irradiation age is around 5,000 years for 100 μm-sized particles at 1 AU (up to 100,000 years of solar system evolution). This calculation takes into account vertical particle migration, which results in their residence in the upper layers of the disk (where they are more effectively irradiated) due to the gas drag and turbulence motion. In any case, the nebula disappeared in a few Myr (Beckwith & Sargent, 1996; Wyatt et al., 2003) and therefore, grains in this region of the disk end up being irradiated.

If the solar wind implantation scenario were correct, it would imply that a fraction of Earth's highly volatile elements (at least He, Ne, Ar, and likely H) were incorporated into Earth's precursor grains in the first few Myr of the solar system. Solar wind implantation onto these grains induced the formation of a rim with a distinct chemical composition compared to the original grain. In particular, the rim is enriched in Si, S, and Fe and depleted in Ca and Mg (Bradley, 1994; Carrez et al., 2002). The discovery of such anomalies in planetary objects would substantiate this scenario as the likely origin of highly volatile elements in the terrestrial planets.

4.4. The Late Veneer Hypothesis

As already mentioned in sections 2 and 4.1, at least one other noble gas source is required to account for the noble gas isotopic composition of the atmosphere. Two outer solar system sources could explain the

lower $^{20}Ne/^{22}Ne$ ratio of the atmosphere compared with that of the mantle: comets and carbonaceous chondrites, both of which are expected to have low $^{20}Ne/^{22}Ne$ ratios. A late veneer of carbonaceous chondrites was advocated to explain the origin of some highly and moderately volatile elements (Albarède, 2009; Halliday, 2013; Hirschmann & Dasgupta, 2009; Marty, 2012). Comets could also have contributed to the Earth's atmospheric noble gas budget in a late veneer phase (Dauphas, 2003; Halliday, 2013; Marty et al., 2016, 2017). Marty et al. (2017) estimated that comets contributed to 22% of the atmospheric xenon budget. Comets could hence be an important source of atmospheric noble gases but their contribution to major volatiles (H, C, and N) was likely very limited (up to a very few percent) because of very different isotopic compositions for D/H, $^{15}N/^{14}N$ ratios and elemental composition (Balsiger et al., 2015; Marty, 2012; Marty et al., 2016).

If we consider that the neon in the Earth's atmosphere comes from a mixture of carbonaceous chondrites (or cometary material) having a low $^{20}Ne/^{22}Ne$ ratio of about 8.2 (e.g., Mazor et al., 1970, and also refer to section 2.3) and degassing mantle with a $^{20}Ne/^{22}Ne$ ratio of 12.65, then the proportion of carbonaceous chondrite-derived Ne (or cometary) in the atmosphere is about 64%. The calculated atmospheric $^{22}Ne/^{36}Ar$ ratio would be 0.051, similar to the present-day atmospheric value (0.053) (Figure 6).

A late veneer could hence explain the atmospheric $^{20}Ne/^{22}Ne$ ratio but one may ask whether a mixture of solar-wind-implanted gases and chondritic/cometary gases is also valid for atmospheric argon or not. We have shown that the mantle $^{38}Ar/^{36}Ar$ ratio (0.1887 ± 0.006; Péron et al., 2017) is close to the atmospheric ratio (0.1880) and that lunar soils also have a $^{38}Ar/^{36}Ar$ ratio similar to the atmospheric ratio, except ilmenites that show a higher ratio of around 0.1933 ± 0.0024. The mantle $^{38}Ar/^{36}Ar$ ratio may also be explained via solar wind implantation. However, carbonaceous chondrites have a low $^{38}Ar/^{36}Ar$ ratio (about 0.1842 ± 0.0044; Mazor et al., 1970) and so mixing mantle gases and carbonaceous chondrites yields a lower $^{38}Ar/^{36}Ar$ ratio (0.1844) than the atmospheric value. For the latter calculation, the proportion of chondritic argon would be 95% given the $^{22}Ne/^{36}Ar$ ratio (0.051) calculated just above and the $^{22}Ne/^{36}Ar$ ratios of the mantle and carbonaceous chondrites in Table 4. But it is important to note that the uncertainties on the carbonaceous compositions from Mazor et al. (1970) are large and that this composition seems not well constrained. If we consider that the late veneer chondritic material has rather a $^{38}Ar/^{36}Ar$ ratio of 0.1873 ± 0.0007 (composition of phase Q; Busemann et al., 2000), then such mixing gives a range of 0.1867–0.1880 for the $^{38}Ar/^{36}Ar$ ratio considering the uncertainties on Phase Q composition. But phase Q is only a small fraction of chondrites (Busemann et al., 2000). Therefore, it is unlikely that a late veneer has the argon composition of phase Q but rather would have had the argon composition of the bulk material, which may be a mixture of several argon components.

So the scenario of mixing mantle gases having a solar-wind-implanted signature with gases from a late veneer used to explain the neon atmospheric composition could also account for the argon isotopic $^{38}Ar/^{36}Ar$ ratio. But the above calculations depend on the argon carbonaceous chondrites composition, which is not known precisely. So we cannot conclude on it.

It is also important to remember that the mantle $^{38}Ar/^{36}Ar$ ratio is very hard to measure because of the low abundance of ^{38}Ar and so it is not yet well constrained. Moreover, atmospheric argon could be recycled into the mantle (Holland & Ballentine, 2006; Jackson et al., 2013; Kendrick et al., 2011; Smye et al., 2017) thereby erasing the primitive mantle signature. The case of argon is less straightforward since isotopic differences between chondrites, the mantle, the atmosphere, and lunar soils are very small and so more work is required to explain the nature of the argon isotopic signature (in particular refining the uncertainties on the A component's $^{38}Ar/^{36}Ar$ ratio, Table 4).

5. Conclusion

We have compared the neon and argon isotopic and elemental compositions of the Earth with that of lunar soils, IDPs, micrometeorites, solar wind, and chondrites to discuss three models for the origin of noble gases on Earth (solar wind implantation, solar gas dissolution, and the late veneer model).

We showed that the plume mantle source neon and argon compositions are close to that of the solar-wind-implanted signature (component B). We present a calculation showing that the measured $^{20}Ne/^{22}Ne$ ratio in OIB, inferred to be representative of the plume mantle sources, seems close to the primitive mantle's

$^{20}Ne/^{22}Ne$ ratio. Therefore, mantle neon seems different from solar neon and the scenario of solar nebula gas dissolution into a magma ocean seems unlikely to explain Earth's neon composition. The latter scenario cannot be however totally excluded. Existing evidence favors the solar wind irradiation model to account for the origin of light noble gases (He and Ne) in the mantle, a scenario that may also account for mantle's H budget. This would imply that these light volatiles were incorporated into the Earth's precursor grains in the first few Myr of solar system formation, and survived (at least partially) to subsequent heating attending accretion. A few percent of such grains are needed to account for the Earth's light gas budget. The neon atmospheric composition can be explained by mixing 36% of gases from the mantle having the B composition and 64% of gases from a chondritic (or cometary?) source delivered to the Earth in a late veneer phase (unless a fraction of atmospheric neon was lost from a still-unknown process as mentioned in section 2.3).

The case of Argon is less straightforward and more work is needed to resolve the issue of argon recycling into the mantle via subduction.

Acknowledgments
The data supporting the conclusions can be found in Tables 1 and 4 and in the references. The authors thank Nicole Stroncik, two other anonymous reviewers, and the Editor for constructive reviews that greatly improved the manuscript. S.P. wants to acknowledge the financial support from L'Oréal-UNESCO *For Women in Science* France 2017 fellowship. A.A. thanks PETROBRAS, Adriano R. Viana, and Laurent Geoffroy for the financial support of the sampling in Greenland through the program VOLCABASIN. The authors are also very grateful to Mark D. Kurz and Paolo Sossi for constructive comments and discussions on the first versions of this manuscript. We acknowledge the financial support of the UnivEarthS Labex program at Sorbonne Paris Cité (ANR-10-LABX-0023 and ANR-11-IDEX-0005-02). This is IPGP contribution number 3932.

References

Albarède, F. (2009). Volatile accretion history of the terrestrial planets and dynamic implications. *Nature*, *461*, 1227–1233. https://doi.org/10.1038/nature08477

Allègre, C. J., Staudacher, T., Sarda, P., & Kurz, M. D. (1983). Constraints on evolution of Earth's mantle from rare gas systematics. *Nature*, *303*, 762–766. https://doi.org/10.1038/303762a0

Asaduzzaman, A., Muralidharan, K., & Ganguly, J. (2015). Incorporation of water into olivine during nebular condensation: Insights from density functional theory and thermodynamics, and implications for phyllosilicate formation and terrestrial water inventory. *Meteoritics & Planetary Science*, *50*, 578–589. https://doi.org/10.1111/maps.12409

Asaduzzaman, A. M., Laref, S., Deymier, P. A., Runge, K., Cheng, H. P., Muralidharan, K., et al. (2013). A first-principles characterization of water adsorption on forsterite grains. *Philosophical Transactions of the Royal Society A: Mathematical, Physical and Engineering Sciences*, *371*, 20110582. https://doi.org/10.1098/rsta.2011.0582

Bajo, K-I., Akaida, T., Ohashi, N., Noguchi, T., Nakamura, T., Nakamura, Y., et al. (2012). Single grain noble gas analysis of Antarctic micrometeorites by stepwise heating method with a newly constructed miniature furnace. *Earth, Planets and Space*, *63*, 9. https://doi.org/10.5047/eps.2011.08.001

Ballentine, C., & Barfod, D. (2000). The origin of air-like noble gases in MORB and OIB. *Earth and Planetary Science Letters*, *180*, 39–48. https://doi.org/10.1016/S0012-821X(00)00161-8

Ballentine, C. J., Marty, B., Lollar, B. S., & Cassidy, M. (2005). Neon isotopes constrain convection and volatile origin in the Earth's mantle. *Nature*, *433*, 33–38. https://doi.org/10.1038/nature03182

Balsiger, H., Altwegg, K., Bar-Nun, A., Berthelier, J.-J., Bieler, A., Bochsler, P., et al. (2015). Detection of argon in the coma of comet ^{67}P/Churyumov-Gerasimenko. *Science Advances*, *1*, e1500377. https://doi.org/10.1126/sciadv.1500377

Beckwith, S. V. W., & Sargent, A. I. (1996). Circumstellar disks and the search for neighbouring planetary systems. *Nature*, *383*, 139–144. https://doi.org/10.1038/383139a0

Benkert, J.-P., Baur, H., Signer, P., & Wieler, R. (1993). He, Ne, and Ar from the solar wind and solar energetic particles in lunar ilmenites and pyroxenes. *Journal of Geophysical Research*, *98*, 13147–13162. https://doi.org/10.1029/93JE01460

Black, D. C. (1970). Trapped helium-neon isotopic correlations in gas-rich meteorites and carbonaceous chondrites. *Geochimica et Cosmochimica Acta*, *34*, 132–140. https://doi.org/10.1016/0016-7037(70)90158-4

Black, D. C. (1971). Trapped neon-argon isotopic correlations in gas rich meteorites and carbonaceous chondrites. *Geochimica et Cosmochimica Acta*, *35*, 230–235. https://doi.org/10.1016/0016-7037(71)90060-3

Black, D. C. (1972). On the origins of trapped helium, neon and argon isotopic variations in meteorites—I. Gas-rich meteorites, lunar soil and breccia. *Geochimica et Cosmochimica Acta*, *36*, 347–375. https://doi.org/10.1016/0016-7037(72)90029-4

Black, D. C., & Pepin, R. O. (1969). Trapped neon in meteorites—II. *Earth and Planetary Science Letters*, *6*, 395–405. https://doi.org/10.1016/0012-821X(69)90190-3

Bogard, D. D., & Hirsch, W. C. (1975). Noble gas studies on grain size separates of Apollo 15 and 16 deep drill cores. In *Proceedings of the 6th Lunar Science Conference*. New York, NY: Pergamon.

Bogard, D. D., Nyquist, L. E., & Hirsch, W. C. (1974). Noble gases in Apollo 17 fines - Mass fractionation effects in trapped Xe and Kr. In *Proceedings of the 5th Lunar Science Conference*. New York, NY: Pergamon.

Bogard, D. D., Nyquist, L. E., Hirsch, W. C., & Moore, D. R. (1973). Trapped solar and cosmogenic noble gas abundances in Apollo 15 and 16 deep drill samples. *Earth and Planetary Science Letters*, *21*, 52–69. https://doi.org/10.1016/0012-821X(73)90225-2

Bradley, J. P. (1994). Chemically anomalous, preaccretionally irradiated grains in interplanetary dust from comets. *Science*, *265*, 925. https://doi.org/10.1126/science.265.5174.925

Bradley, J. P., Ishii, H. A., Gillis-Davis, J. J., Ciston, J., Nielsen, M. H., Bechtel, H. A., et al. (2014). Detection of solar wind-produced water in irradiated rims on silicate minerals. *Proceedings of the National Academy of Sciences of the United States of America*, *111*, 1732–1735. https://doi.org/10.1073/pnas.1320115111

Burnard, P. (1999). The bubble-by-bubble volatile evolution of two mid-ocean ridge basalts. *Earth and Planetary Science Letters*, *174*, 199–211. https://doi.org/10.1016/S0012-821X(99)00254-X

Burnard, P., Graham, D., & Turner, G. (1997). Vesicle-specific noble gas analyses of "popping rock": Implications for primordial noble gases in the Earth. *Science*, *276*, 568–571. https://doi.org/10.1126/science.276.5312.568

Busemann, H., Baur, H., & Wieler, R. (2000). Primordial noble gases in "phase Q" in carbonaceous and ordinary chondrites studied by closed-system stepped etching. *Meteoritics & Planetary Science*, *35*, 949–973. https://doi.org/10.1111/j.1945-5100.2000.tb01485.x

Carrez, P., Demyk, K., Cordier, P., Gengembre, L., Grimblot, J., d'Hendecourt, L., et al. (2002). Low-energy helium ion irradiation-induced amorphization and chemical changes in olivine: Insights for silicate dust evolution in the interstellar medium. *Meteoritics & Planetary Science*, *37*, 1599–1614. https://doi.org/10.1111/j.1945-5100.2002.tb00814.x

Colin, A., Burnard, P., & Marty, B. (2013). Mechanisms of magma degassing at mid-oceanic ridges and the local volatile composition (^4He–$^{40}Ar^*$–CO_2) of the mantle by laser ablation analysis of individual MORB vesicles. *Earth and Planetary Science Letters*, *361*, 183–194. https://doi.org/10.1016/j.epsl.2012.10.022

Colin, A., Moreira, M., Gautheron, C., & Burnard, P. (2015). Constraints on the noble gas composition of the deep mantle by bubble-by-bubble analysis of a volcanic glass sample from Iceland. *Chemical Geology*, *417*, 173–183. https://doi.org/10.1016/j.chemgeo.2015.09.020

Coltice, N., Moreira, M., Hernlund, J., & Labrosse, S. (2011). Crystallization of a basal magma ocean recorded by helium and neon. *Earth and Planetary Science Letters*, *308*, 193–199. https://doi.org/10.1016/j.epsl.2011.05.045

Dauphas, N. (2003). The dual origin of the terrestrial atmosphere. *Icarus*, *165*, 326–339. https://doi.org/10.1016/S0019-1035(03)00198-2

Dauphas, N., Chen, J. H., Zhang, J., Papanastassiou, D. A., Davis, A. M., & Travaglio, C. (2014). Calcium-48 isotopic anomalies in bulk chondrites and achondrites: Evidence for a uniform isotopic reservoir in the inner protoplanetary disk. *Earth and Planetary Science Letters*, *407*, 96–108. https://doi.org/10.1016/j.epsl.2014.09.015

Djouadi, Z., Robert, F., Le Sergeant D'hendecourt, L., Mostefaoui, S., Leroux, H., Jones, A. P., et al. (2011). Hydroxyl radical production and storage in analogues of amorphous interstellar silicates: A possible "wet" accretion phase for inner telluric planets. *Astronomy & Astrophysics*, *531*, A96. https://doi.org/10.1051/0004-6361/201116722

Drake, M. J. (2005). Origin of water in the terrestrial planets. *Meteoritics & Planetary Science*, *40*, 519–527. https://doi.org/10.1111/j.1945-5100.2005.tb00960.x

Drake, M. J., & Righter, K. (2002). Determining the composition of the Earth. *Nature*, *416*, 39–44. https://doi.org/10.1038/416039a

Eberhardt, P., Geiss, J., Graf, H., Grögler, N., Krähenbühl, U., Schwaller, H., et al. (1970). Trapped solar wind noble gases, exposure age and K/Ar age in Apollo 11 lunar fine material. In *Proceedings of the 2nd Apollo 11 Lunar Science Conference* (pp. 1037–1070). New York, NY: Pergamon.

Eberhardt, P., Geiss, J., Graf, H., Grögler, N., Mendia, M. D., Mörgeli, M., et al. (1972). Trapped solar wind noble gases in Apollo 12 lunar fines 12001 and Apollo 11 breccia 10046. In *Proceedings of the Third Lunar Science Conference* (Vol. 3, pp. 1821–1856). Cambridge, MA: MIT Press.

Eugster, O. (1985). Multistage exposure history of the 74261 soil constituents. *Journal of Geophysical Research*, *90*, 95–102. https://doi.org/10.1029/JB090iS01p00095

Eugster, O., Grögler, N., Mendia, M. D., Eberhardt, P., & Geiss, J. (1973). Trapped solar wind noble gases and exposure age of Luna 16 lunar fines. *Geochimica et Cosmochimica Acta*, *37*, 1991–2003. https://doi.org/10.1016/0016-7037(73)90001-X

French, S. W., & Romanowicz, B. (2015). Broad plumes rooted at the base of the Earth's mantle beneath major hotspots. *Nature*, *525*, 95. https://doi.org/10.1038/nature14876

Funkhouser, J. G., Schaeffer, O. A., Bogard, D. D., & Zähringer, J. (1970). Gas analysis of the lunar surface. In A. A. Levinson (Ed.), *Proceedings of the Apollo 11 Lunar Science Conference* (pp. 1111–1116). New York, NY: Pergamon.

Füri, E., Aléon-Toppani, A., Marty, B., Libourel, G., & Zimmermann, L. (2013). Effects of atmospheric entry heating on the noble gas and nitrogen content of micrometeorites. *Earth and Planetary Science Letters*, *377*, 1–12. https://doi.org/10.1016/j.epsl.2013.07.031

Füri, E., Barry, P. H., Taylor, L. A., & Marty, B. (2015). Indigenous nitrogen in the Moon: Constraints from coupled nitrogen–noble gas analyses of mare basalts. *Earth and Planetary Science Letters*, *431*, 195–205. https://doi.org/10.1016/j.epsl.2015.09.022

Füri, E., Deloule, E., Gurenko, A., & Marty, B. (2014). New evidence for chondritic lunar water from combined D/H and noble gas analyses of single Apollo 17 volcanic glasses. *Icarus*, *229*, 109–120. https://doi.org/10.1016/j.icarus.2013.10.029

Geiss, J., Bühler, F., Cerutti, H., Eberhardt, P., Filleux, C., Meister, J., et al. (2004). The Apollo SWC experiment: Results, conclusions, consequences. *Space Science Reviews*, *110*, 307–335. https://doi.org/10.1023/B:SPAC.0000023409.54469.40

Graham, D. W., Larsen, L. M., Hanan, B. B., Storey, M., Pedersen, A. K., & Lupton, J. E. (1998). Helium isotope composition of the early Iceland mantle plume inferred from the Tertiary picrites of West Greenland. *Earth and Planetary Science Letters*, *160*, 241–255. https://doi.org/10.1016/S0012-821X(98)00083-1

Grevesse, N., Asplund, M., & Sauval, A. J. (2005). The new solar chemical composition. In G. Alecian, O. Richard, & S. Vauclair (Eds.), *Element stratification in stars: 40 years of atomic diffusion. EAS publications series* (Vol. 17, pp. 21–30). https://doi.org/10.1051/eas:2005095

Grimberg, A., Baur, H., Bochsler, P., Bühler, F., Burnett, D. S., Hays, C. C., et al. (2006). Solar wind neon from genesis: Implications for the lunar noble gas record. *Science*, *314*, 1133–1135. https://doi.org/10.1126/science.1133568

Grimberg, A., Baur, H., Bühler, F., Bochsler, P., & Wieler, R. (2008). Solar wind helium, neon and argon isotopic and elemental composition: Data from the metallic glass flown on NASA's Genesis mission. *Geochimica et Cosmochimica Acta*, *72*, 626–645. https://doi.org/10.1016/j.gca.2007.10.017

Halliday, A. (2013). The origins of volatiles in the terrestrial planets. *Geochimica et Cosmochimica Acta*, *105*, 146–171. https://doi.org/10.1016/j.gca.2012.11.015

Harper, C. L., & Jacobsen, S. B. (1996). Noble gases and Earth's accretion. *Science*, *273*, 1814–1818. https://doi.org/10.1126/science.273.5283.1814

Heber, V. S., Baur, H., Bochsler, P., McKeegan, K. D., Neugebauer, M., Reisenfeld, D. B., et al. (2012). Isotopic mass fractionation of solar wind: Evidence from fast and slow solar wind collected by the genesis mission. *The Astrophysical Journal*, *759*, 121. https://doi.org/10.1088/0004-637x/759/2/121

Heber, V. S., Wieler, R., Baur, H., Olinger, C., Friedmann, A., & Burnett, D. S. (2009). Noble gas composition of the solar wind as collected by the Genesis mission. *Geochimica et Cosmochimica Acta*, *73*, 7414–7432. https://doi.org/10.1016/j.gca.2009.09.013

Heymann, D., Lakatos, S., & Walton, J. R. (1973). Inert gases in a terra sample: Measurements in six grain-size fractions and two single particles from Luna 20. *Geochimica et Cosmochimica Acta*, *37*, 875–885. https://doi.org/10.1016/0016-7037(73)90185-3

Heymann, D., & Yaniv, A. (1970). Inert gases in the fines from the sea of tranquility. In *Proceedings of the Apollo 11 Lunar Science Conference* (pp. 1247–1259). New York, NY: Pergamon.

Heymann, D., Yaniv, A., & Lakatos, S. (1972). Inert gases in twelve particles and one "dust" sample from Luna 16. *Earth and Planetary Science Letters*, *13*, 400–406. https://doi.org/10.1016/0012-821X(72)90115-X

Hintenberger, H., Weber, H. W., Voshage, H., Wänke, H., Begemann, F., & Wlotzka, F. (1970). Concentrations and isotopic abundances of the rare gases, hydrogen and nitrogen in lunar matter. In A. A. Levinson (Ed.), *Proceedings of the Apollo 11 Lunar Science Conference* (pp. 1269–1282). New York, NY: Pergamon.

Hirschmann, M. M. (2016). Constraints on the early delivery and fractionation of Earth's major volatiles from C/H, C/N, and C/S ratios. *American Mineralogist*, *101*, 540. https://doi.org/10.2138/am-2016-5452

Hirschmann, M. M., & Dasgupta, R. (2009). The H/C ratios of Earth's near-surface and deep reservoirs, and consequences for deep Earth volatile cycles. *Chemical Geology*, *262*, 4–16. https://doi.org/10.1016/j.chemgeo.2009.02.008

Holland, G., & Ballentine, C. J. (2006). Seawater subduction controls the heavy noble gas composition of the mantle. *Nature*, *441*, 186–191. https://doi.org/10.1038/nature04761

Honda, M., McDougall, I., Patterson, D. B., Doulgeris, A., & Clague, D. (1991). Possible solar noble-gas component in Hawaiian basalts. *Nature*, *349*, 149–151. https://doi.org/10.1038/349149a0

Honda, M., McDougall, I., Patterson, D. B., Doulgeris, A., & Clague, D. (1993). Noble gases in submarine pillow basalt glasses from Loihi and Kilauea, Hawaii: A solar component in the Earth. *Geochimica et Cosmochimica Acta*, *57*, 859–874. https://doi.org/10.1016/0016-7037(93)90174-U

Hopp, J., & Trieloff, M. (2008). Helium deficit in high-^{3}He/^{4}He parent magmas: Predegassing fractionation, not a "helium paradox. *Geochemistry, Geophysics, Geosystems*, *9*, Q03009. https://doi.org/10.1029/2007GC001833

Hopp, J., Trieloff, M., & Altherr, R. (2004). Neon isotopes in mantle rocks from the Red Sea region reveal large-scale plume-lithosphere interaction. *Earth and Planetary Science Letters*, *219*, 61–76. https://doi.org/10.1016/S0012-821X(03)00691-5

Hübner, W., Kirsten, T., & Kiko, J. (1975). Rare gases in Apollo 17 soils with emphasis on analysis of size and mineral fractions of soil 74241. *Abstracts of the Lunar and Planetary Science Conference*, *5*, 369.

Hudson, B., Flynn, G. J., Fraundorf, P., Hohenberg, C. M., & Shirck, J. (1981). Noble gases in stratospheric dust particles: Confirmation of extraterrestrial origin. *Science*, *211*, 383. https://doi.org/10.1126/science.211.4480.383

Hunten, D. M., Pepin, R. O., & Walker, J. C. B. (1987). Mass fractionation in hydrodynamic escape. *Icarus*, *43*, 22–28. https://doi.org/10.1016/0019-1035(87)90022-4

Jackson, C. R. M., Parman, S. W., Kelley, S. P., & Cooper, R. F. (2013). Noble gas transport into the mantle facilitated by high solubility in amphibole. *Nature Geoscience*, *6*, 562–565. https://doi.org/10.1038/ngeo1851

Jackson, M. G., Kurz, M. D., & Hart, S. R. (2009). Helium and neon isotopes in phenocrysts from Samoan lavas: Evidence for heterogeneity in the terrestrial high ^{3}He/^{4}He mantle. *Earth and Planetary Science Letters*, *287*, 519–528. https://doi.org/10.1016/j.epsl.2009.08.039

Jaupart, E., Charnoz, S., & Moreira, M. (2017). Primordial atmosphere incorporation in planetary embryos and the origin of Neon in terrestrial planets. *Icarus*, *293*, 199–205. https://doi.org/10.1016/j.icarus.2017.04.022

Javoy, M. (1995). The integral Enstatite Chondrite model of the Earth. *Geophysical Research Letters*, *22*, 2219–2222. https://doi.org/10.1029/95GL02015

Javoy, M., Kaminski, E., Guyot, F., Andrault, D., Sanloup, C., Moreira, M., et al. (2010). The chemical composition of the Earth: Enstatite chondrite models. *Earth and Planetary Science Letters*, *293*, 259–268. https://doi.org/10.1016/j.epsl.2010.02.033

Jordan, J. L., Heymann, D., & Lakatos, S. (1974). Inert gas patterns in the regolith at the Apollo 15 landing site. *Geochimica et Cosmochimica Acta*, *38*, 65–78. https://doi.org/10.1016/0016-7037(74)90195-1

Kehm, K., Flynn, G. J., & Hohenberg, C. M. (2006). Noble gas space exposure ages of individual interplanetary dust particles. *Meteoritics & Planetary Science*, *41*, 1199–1217. https://doi.org/10.1111/j.1945-5100.2006.tb00516.x

Kendrick, M. A., Scambelluri, M., Honda, M., & Phillips, D. (2011). High abundances of noble gas and chlorine delivered to the mantle by serpentine subduction. *Nature Geoscience*, *4*, https://doi.org/10.1038/ngeo1270

Kirsten, T., Horn, P., & Kiko, J. (1973). ^{39}Ar–^{40}Ar dating and rare gas analysis of Apollo 16 rocks and soils. *Proceedings of the Lunar and Planetary Science Conference*, *4*, 1757.

Kirsten, T., Müller, O., Steinbrunn, F., & Zähringer, J. (1970). Study of distribution and variations of rare gases in lunar material by a microprobe technique. *Geochimica et Cosmochimica Acta Supplement*, *1*, 1331–1343.

Kurz, M. D., Curtice, J., Fornari, D., Geist, D., & Moreira, M. (2009). Primitive neon from the center of the Galápagos hotspot. *Earth and Planetary Science Letters*, *286*, 23–34. https://doi.org/10.1016/j.epsl.2009.06.008

Kurz, M. D., Jenkins, W. J., & Hart, S. R. (1982). Helium isotopic systematics of oceanic islands and mantle heterogeneity. *Nature*, *297*, 43–47. https://doi.org/10.1038/297043a0

Kurz, M. D., Rowland, S. K., Curtice, J., Saal, A. E., & Naumann, T. (2014). Eruption rates for Fernandina volcano: A new chronology at the Galápagos Hotspot Center. in K. S. Harpp, E. Mittelstaedt, N. d'Ozouville, & D. W. Graham (Eds.), *The Galápagos: A natural laboratory for the Earth sciences* (pp. 41–54). Hoboken, NJ: John Wiley. https://doi.org/10.1002/9781118852538.ch4

Lee, J.-Y., Marti, K., Severinghaus, J. P., Kawamura, K., Yoo, H.-S., Lee, J., et al. (2006). A redetermination of the isotopic abundances of atmospheric Ar. *Geochimica et Cosmochimica Acta*, *70*, 4507–4512. https://doi.org/10.1016/j.gca.2006.06.1563

Marty, B. (2012). The origins and concentrations of water, carbon, nitrogen and noble gases on Earth. *Earth and Planetary Science Letters*, *313–314*, 56–66. https://doi.org/10.1016/j.epsl.2011.10.040

Marty, B., Altwegg, K., Balsiger, H., Bar-Nun, A., Bekaert, D. V., Berthelier, J. J., et al. (2017). Xenon isotopes in ^{67}P/Churyumov-Gerasimenko show that comets contributed to Earth's atmosphere. *Science*, *356*, 1069–1072. https://doi.org/10.1126/science.aal3496

Marty, B., Avice, G., Sano, Y., Altwegg, K., Balsiger, H., Hässig, M., et al. (2016). Origins of volatile elements (H, C, N, noble gases) on Earth and Mars in light of recent results from the ROSETTA cometary mission. *Earth and Planetary Science Letters*, *441*, 91–102. https://doi.org/10.1016/j.epsl.2016.02.031

Marty, B., Robert, P., & Zimmermann, L. (2005). Nitrogen and noble gases in micrometeorites. *Meteoritics & Planetary Science*, *40*, 881–894. https://doi.org/10.1111/j.1945-5100.2005.tb00161.x

Mazor, E., Heymann, D., & Anders, E. (1970). Noble gases in carbonaceous chondrites. *Geochimica et Cosmochimica Acta*, *34*, 781–824. https://doi.org/10.1016/0016-7037(70)90031-1

McKay, D. S., Heiken, G., Basu, A., Blanford, G., Simon, S., Reedy, R., et al. (1991). The lunar regolith. In G. Heiken, D. Vaniman, & B. M. French (Eds.), *Lunar sourcebook* (pp. 285–356). Cambridge, UK: Cambridge University Press.

Meshik, A., Hohenberg, C., Burnett, D., & Pravdivtseva, O. (2012). *Measuring the isotopic composition of solar wind noble gases*. London, UK: INTECH Open Access. https://doi.org/10.5772/37908[WorldCat]

Meshik, A., Hohenberg, C., Pravdivtseva, O., & Burnett, D. (2014). Heavy noble gases in solar wind delivered by Genesis mission. *Geochimica et Cosmochimica Acta*, *127*, 326–347. https://doi.org/10.1016/j.gca.2013.11.030

Meshik, A., Mabry, J., Hohenberg, C., Marrocchi, Y., Pravdivtseva, O., Burnett, D., et al. (2007). Constraints on neon and argon isotopic fractionation in solar wind. *Science*, *318*, 433–435. https://doi.org/10.1126/science.1145528

Michael, P. J., & Cornell, W. C. (1998). Influence of spreading rate and magma supply on crystallization and assimilation beneath mid-ocean ridges: Evidence from chlorine and major element chemistry of mid-ocean ridge basalts. *Journal of Geophysical Research*, *103*, 18325–18356. https://doi.org/10.1029/98JB00791

Mizuno, H., Nakazawa, K., & Hayashi, C. (1980). Dissolution of the primordial rare gases into the molten Earth's mantle. *Earth and Planetary Science Letters*, *50*, 202–210. https://doi.org/10.1016/0012-821X(80)90131-4

Morbidelli, A., Chambers, J., Lunine, J., Petit, J., Robert, F., Valsecchi, G., et al. (2000). Source regions and timescales for the delivery of water to the Earth. *Meteoritics & Planetary Science*, *35*, 1309–1320. https://doi.org/10.1111/j.1945-5100.2000.tb01518.x

Moreira, M. (2013). Noble gas constraints on the origin and evolution of Earth's volatiles. *Geochemical Perspectives*, *2*, 229–403. https://doi.org/10.7185/geochempersp.2.2

Moreira, M., & Allègre, C. J. (1998). Helium–neon systematics and the structure of the mantle. *Chemical Geology*, *147*, 53–59. https://doi.org/10.1016/S0009-2541(97)00171-X

Moreira, M., Blusztajn, J., Curtice, J., Hart, S., Dick, H., & Kurz, M. D. (2003). He and Ne isotopes in oceanic crust: Implications for noble gas recycling in the mantle. *Earth and Planetary Science Letters*, *216*, 635–643. https://doi.org/10.1016/S0012-821X(03)00554-5

Moreira, M., & Charnoz, S. (2016). The origin of the neon isotopes in chondrites and on Earth. *Earth and Planetary Science Letters*, *433*, 249–256. https://doi.org/10.1016/j.epsl.2015.11.002

Moreira, M., Kunz, J., & Allègre, C. J. (1998). Rare gas systematics on popping rock: Estimates of isotopic and elemental compositions in the upper mantle. *Science*, *279*, 1178–1181. https://doi.org/10.1126/science.279.5354.1178

Moreira, M., Staudacher, T., Sarda, P., Schilling, J.-G., & Allègre, C. J. (1995). A primitive plume neon component in MORB: The Shona ridge-anomaly, South Atlantic (51–52°S). *Earth and Planetary Science Letters*, *133*, 367–377. https://doi.org/10.1016/0012-821X(95)00080-V

Moreira, M. A., & Kurz, M. D. (2013). Noble gases as tracers of mantle processes and magmatic degassing. In P. Burnard (Ed.), *The noble gases as geochemical tracers* (pp. 371–391). Berlin, Germany: Springer. https://doi.org/10.1007/978-3-642-28836-4_12

Mortimer, J., Verchovsky, A. B., & Anand, M. (2016). Predominantly non-solar origin of nitrogen in lunar soils. *Geochimica et Cosmochimica Acta*, *193*, 36–53. https://doi.org/10.1016/j.gca.2016.08.006

Mortimer, J., Verchovsky, A. B., Anand, M., Gilmour, I., & Pillinger, C. T. (2015). Simultaneous analysis of abundance and isotopic composition of nitrogen, carbon, and noble gases in lunar basalts: Insights into interior and surface processes on the Moon. *Icarus*, *255*, 3–17. https://doi.org/10.1016/j.icarus.2014.10.006

Mukhopadhyay, S. (2012). Early differentiation and volatile accretion recorded in deep mantle neon and xenon. *Nature*, *486*, 101–104. https://doi.org/10.1038/nature11141

Nier, A. O., & Schlutter, D. J. (1990). Helium and neon isotopes in stratospheric particles. *Meteoritics*, *25*, 263–267. https://doi.org/10.1111/j.1945-5100.1990.tb00710.x

Nier, A. O., & Schlutter, D. J. (1992). Extraction of helium from individual interplanetary dust particles by step-heating. *Meteoritics*, *27*, 166–173. https://doi.org/10.1111/j.1945-5100.1992.tb00744.x

O'Brien, D. P., Walsh, K. J., Morbidelli, A., Raymond, S. N., & Mandell, A. M. (2014). Water delivery and giant impacts in the 'Grand Tack' scenario. *Icarus*, *239*, 74–84. https://doi.org/10.1016/j.icarus.2014.05.009

Okazaki, R., Noguchi, T., Tsujimoto, S-I., Tobimatsu, Y., Nakamura, T., Ebihara, M., et al. (2015). Mineralogy and noble gas isotopes of micrometeorites collected from Antarctic snow. *Earth, Planets and Space*, *67*, 90. https://doi.org/10.1186/s40623-015-0261-8

Osawa, T., & Nagao, K. (2002a). Noble gas compositions of Antarctic micrometeorites collected at the Dome Fuji Station in 1996 and 1997. *Meteoritics & Planetary Science*, *37*, 911–936. https://doi.org/10.1111/j.1945-5100.2002.tb00867.x

Osawa, T., & Nagao, K. (2002b). On low noble gas concentrations in Antarctic micrometeorites collected from Kuwagata Nunatak in the Yamato Meteorite Ice Field. *Antarctic Meteorite Research*, *15*, 165–177.

Osawa, T., Nagao, K., Nakamura, T., & Takaoka, N. (2000). Noble gas measurement in individual micrometeorites using laser gas-extraction system. *Antarctic Meteorite Research*, *13*, 322–341.

Osawa, T., Nakamura, T., & Nagao, K. (2003). Noble gas isotopes and mineral assemblages of Antarctic micrometeorites collected at the meteorite ice field around the Yamato Mountains. *Meteoritics & Planetary Science*, *38*, 1627–1640. https://doi.org/10.1111/j.1945-5100.2003.tb00005.x

Parai, R., & Mukhopadhyay, S. (2015). The evolution of MORB and plume mantle volatile budgets: Constraints from fission Xe isotopes in Southwest Indian Ridge basalts. *Geochemistry, Geophysics, Geosystems*, *16*, 719–735. https://doi.org/10.1002/2014GC005566

Patzer, A., & Schultz, L. (2002). Noble gases in enstatite chondrites II: The trapped component. *Meteoritics & Planetary Science*, *37*, 601–612. https://doi.org/10.1111/j.1945-5100.2002.tb00841.x

Pepin, R. O. (1967). Trapped neon in meteorites. *Earth and Planetary Science Letters*, *2*, 13–18. https://doi.org/10.1016/0012-821X(67)90165-3

Pepin, R. O., Becker, R. H., & Schlutter, D. J. (1999). Irradiation records in regolith materials. I: Isotopic compositions of solar-wind neon and argon in single lunar mineral grains. *Geochimica et Cosmochimica Acta*, *63*, 2145–2162. https://doi.org/10.1016/S0016-7037(99)00002-2

Pepin, R. O., Nyquist, L. E., Phinney, D., & Black, D. C. (1970). Rare gases in Apollo 11 lunar material. In A. A. Levinson (Ed.), *Proceedings of the Apollo 11 Lunar Science Conference* (pp. 1435–1454). New York, NY: Pergamon.

Pepin, R. O., Palma, R. L., & Schlutter, D. J. (2000). Noble gases in interplanetary dust particles, I: The excess helium-3 problem and estimates of the relative fluxes of solar wind and solar energetic particles in interplanetary space. *Meteoritics & Planetary Science*, *35*, 495–504. https://doi.org/10.1111/j.1945-5100.2000.tb01431.x

Pepin, R. O., Palma, R. L., & Schlutter, D. J. (2001). Noble gases in interplanetary dust particles, II: Excess helium-3 in cluster particles and modeling constraints on interplanetary dust particle exposures to cosmic-ray irradiation. *Meteoritics & Planetary Science*, *36*, 1515–1534. https://doi.org/10.1111/j.1945-5100.2001.tb01843.x

Pepin, R. O., Schlutter, D. J., Becker, R. H., & Reisenfeld, D. B. (2012). Helium, neon, and argon composition of the solar wind as recorded in gold and other Genesis collector materials. *Geochimica et Cosmochimica Acta*, *89*, 62–80. https://doi.org/10.1016/j.gca.2012.04.024

Péron, S., Moreira, M., Colin, A., Arbaret, L., Putlitz, B., & Kurz, M. D. (2016). Neon isotopic composition of the mantle constrained by single vesicle analyses. *Earth and Planetary Science Letters*, *449*, 145–154. https://doi.org/10.1016/j.epsl.2016.05.052

Péron, S., Moreira, M., Putlitz, B., & Kurz, M. D. (2017). Solar wind implantation supplied light volatiles during the first stage of Earth accretion. *Geochemical Perspectives Letters*, *3*, 151–159. https://doi.org/10.7185/geochemlet.1718

Peterson, M. E., Saal, A. E., Kurz, M. D., Hauri, E. H., Blusztajn, J. S., Harpp, K. S., et al. (2017). Submarine basaltic glasses from the Galapagos Archipelago: Determining the volatile budget of the mantle plume. *Journal of Petrology*, *58*, 1419–1450. https://doi.org/10.1093/petrology/egx059

Pető, M. K., Mukhopadhyay, S., & Kelley, K. A. (2013). Heterogeneities from the first 100 million years recorded in deep mantle noble gases from the Northern Lau Back-arc Basin. *Earth and Planetary Science Letters*, *369–370*, 13–23. https://doi.org/10.1016/j.epsl.2013.02.012

Raquin, A., & Moreira, M. (2009). Atmospheric $^{38}Ar/^{36}Ar$ in the mantle: Implications for the nature of the terrestrial parent bodies. *Earth and Planetary Science Letters*, *287*, 551–558. https://doi.org/10.1016/j.epsl.2009.09.003

Raquin, A., Moreira, M., & Guillon, F. (2008). He, Ne and Ar systematics in single vesicles: Mantle isotopic ratios and origin of the air component in basaltic glasses. *Earth and Planetary Science Letters*, *274*, 142–150. https://doi.org/10.1016/j.epsl.2008.07.007

Rider, P. E., Pepin, R. O., & Becker, R. H. (1995). Noble gases and nitrogen released from lunar soils by acid etching. *Geochimica et Cosmochimica Acta*, *59*, 4983–4996. https://doi.org/10.1016/0016-7037(95)00323-1

Sarda, P., Moreira, M., Staudacher, T., Schilling, J.-G., & Allègre, C. J. (2000). Rare gas systematics on the southernmost Mid-Atlantic Ridge: Constraints on the lower mantle and the Dupal source. *Journal of Geophysical Research*, *105*, 5973–5996. https://doi.org/10.1029/1999JB900282

Sarda, P., Staudacher, T., & Allègre, C. J. (1988). Neon isotopes in submarine basalts. *Earth and Planetary Science Letters*, *91*, 73–88. https://doi.org/10.1016/0012-821X(88)90152-5

Schlichting, H. E., & Mukhopadhyay, S. (2018). Atmosphere impact losses. *Space Science Reviews*, *214*, 34. https://doi.org/10.1007/s11214-018-0471-z

Shimizu, K., Saal, A. E., Myers, C. E., Nagle, A. N., Hauri, E. H., Forsyth, D. W., et al. (2016). Two-component mantle melting-mixing model for the generation of mid-ocean ridge basalts: Implications for the volatile content of the Pacific upper mantle. *Geochimica et Cosmochimica Acta*, *176*, 44–80. https://doi.org/10.1016/j.gca.2015.10.033

Smye, A. J., Jackson, C. R. M., Konrad-Schmolke, M., Hesse, M. A., Parman, S. W., Shuster, D. L., et al. (2017). Noble gases recycled into the mantle through cold subduction zones. *Earth and Planetary Science Letters*, *471*, 65–73. https://doi.org/10.1016/j.epsl.2017.04.046

Starkey, N. A., Stuart, F. M., Ellam, R. M., Fitton, J. G., Basu, S., & Larsen, L. M. (2009). Helium isotopes in early Iceland plume picrites: Constraints on the composition of high $^{3}He/^{4}He$ mantle. *Earth and Planetary Science Letters*, *277*, 91–100. https://doi.org/10.1016/j.epsl.2008.10.007

Staudacher, T., & Allègre, C. J. (1988). Recycling of oceanic crust and sediments: The noble gas subduction barrier. *Earth and Planetary Science Letters*, *89*, 173–183. https://doi.org/10.1016/0012-821X(88)90170-7

Stroncik, N. A., & Haase, K. M. (2004). Chlorine in oceanic intraplate basalts: Constraints on mantle sources and recycling processes. *Geology*, *32*, 945–948. https://doi.org/10.1130/g21027.1

Stroncik, N. A., & Niedermann, S. (2016). Atmospheric contamination of the primary Ne and Ar signal in mid-ocean ridge basalts and its implications for ocean crust formation. *Geochimica et Cosmochimica Acta*, *172*, 306–321. https://doi.org/10.1016/j.gca.2015.09.016

Stuart, F. M., Lass-Evans, S., Fitton, J. G., & Ellam, R. M. (2003). High $^{3}He/^{4}He$ ratios in picritic basalts from Baffin Island and the role of a mixed reservoir in mantle plumes. *Nature*, *424*, 57–59. https://doi.org/10.1038/nature01711

Trieloff, M., Kunz, J., Clague, D. A., Harrison, D., & Allègre, C. J. (2000). The nature of pristine noble gases in mantle plumes. *Science*, *288*, 1036–1038. https://doi.org/10.1126/science.288.5468.1036

Trinquier, A., Birck, J.-L., & Allègre, C. J. (2007). Widespread ^{54}Cr heterogeneity in the inner solar system. *The Astrophysical Journal*, *655*, 1179–1185. https://doi.org/10.1086/510360

Tucker, J. M., & Mukhopadhyay, S. (2014). Evidence for multiple magma ocean outgassing and atmospheric loss episodes from mantle noble gases. *Earth and Planetary Science Letters*, *393*, 254–265. https://doi.org/10.1016/j.epsl.2014.02.050

Vogel, N., S., Heber, V., Baur, H., Burnett, D. S., & Wieler, R. (2011). Argon, krypton, and xenon in the bulk solar wind as collected by the Genesis mission. *Geochimica et Cosmochimica Acta*, *75*, 3057–3071. https://doi.org/10.1016/j.gca.2011.02.039

Walsh, K. J., Morbidelli, A., Raymond, S. N., O'Brien, D. P., & Mandell, A. M. (2011). A low mass for Mars from Jupiter's early gas-driven migration. *Nature*, *475*, 206–209. https://doi.org/10.1038/nature10201

Warren, P. H. (2011). Stable-isotopic anomalies and the accretionary assemblage of the Earth and Mars: A subordinate role for carbonaceous chondrites. *Earth and Planetary Science Letters*, *311*, 93–100. https://doi.org/10.1016/j.epsl.2011.08.047

Wieler, R. (2002). Cosmic-ray-produced noble gases in meteorites. *Reviews in Mineralogy and Geochemistry*, *47*(1), 125–170.

Wieler, R., Grimberg, A., & Heber, V. S. (2007). Consequences of the non-existence of the "SEP" component for noble gas geo-and cosmochemistry. *Chemical Geology*, *244*, 382–390. https://doi.org/10.1016/j.chemgeo.2007.06.026

Wyatt, M. C., Dent, W. R. F., & Greaves, J. S. (2003). SCUBA observations of dust around Lindroos stars: Evidence for a substantial submillimetre disc population. *Monthly Notices of the Royal Astronomical Society*, *342*, 876–888. https://doi.org/10.1046/j.1365-8711.2003.06595.x

Yaniv, A., & Heymann, D. (1971). Inert gases from Apollo 11 and Apollo 12 fines: Reversals in the trends of relative element abundances. *Earth and Planetary Science Letters*, *10*, 387–391. https://doi.org/10.1016/0012-821X(71)90085-9

Yatsevich, I., & Honda, M. (1997). Production of nucleogenic neon in the Earth from natural radioactive decay. *Journal of Geophysical Research*, *102*, 10291–10298. https://doi.org/10.1029/97JB00395

Yokochi, R., & Marty, B. (2004). A determination of the neon isotopic composition of the deep mantle. *Earth and Planetary Science Letters*, *225*, 77–88. https://doi.org/10.1016/j.epsl.2004.06.010